Dipolar effective interaction in a fluid of charged spheres near a dielectric plate

J.-N. Aqua*
Laboratoire de Physique,† École Normale Supérieure de Lyon, 46 allée d'Italie, 69364 Lyon, France

F. Cornu
Laboratoire de Physique Théorique,‡ Université Paris–Sud, Bâtiment 210, 91405 Orsay, France
(Received 28 February 2003; published 29 August 2003)

Static correlations in a classical fluid of charged spheres at equilibrium are studied in the vicinity of an insulating wall characterized by its dielectric constant. It is well known that the deformations of screening clouds induced by the presence of the wall result into an effective $f_{\alpha\alpha'}(x,x')/y^3$ interaction in the pair distribution function between two charges e_α and $e_{\alpha'}$ located at distances x and x' from the wall and separated by a large distance y along the wall. We investigate the structure of $f_{\alpha\alpha'}(x,x')$. The method is based on systematic resummations in the Mayer diagrammatics, which are valid both in the bulk and in an inhomogeneous situation. The screened potential ϕ arising in the formalism happens to coincide with the linearized mean-field approximation for the immersion free energy of two external unit charges. ϕ is shown to decay as a *repulsive* $f_\phi(x,x')/y^3$ interaction, whatever the density profiles may be. $f_\phi(x,x')$ takes a factorized dipolar structure $f_\phi(x,x')=\bar{D}_\phi(x)\bar{D}_\phi(x')$ for distances x and x' larger than the maximum of the closest approach distances b_α's to the wall for every species α. Moreover, we devise a reorganization of resummed diagrammatics, which is adequate for the determination of the large-distance behavior of correlations, and we prove that, when all species have the same approach distance b to the wall, $f_{\alpha\alpha'}(x,x';b)=D_\alpha(x)D_{\alpha'}(x')$. In this case, the leading tail of the effective electrostatic interaction between two like charges at the same distance x from a single wall is repulsive. Results are independent of charge magnitudes, of excluded-volume sphere sizes, and of the existence of a surface charge on the wall. It holds whether charges are concentrated at sphere centers or uniformly spread over their surfaces. Comparison is made with an experiment about dilute colloids where the linearized mean-field approximation proves to be relevant. At equilibrium attraction between like charges in confined geometry might arise from purely electrostatic charge-charge interactions only through correlation effects not taken into account in the latter approximation.

DOI: 10.1103/PhysRevE.68.026133 PACS number(s): 05.70.Np, 61.20.Gy, 61.20.Qg

I. INTRODUCTION

A. Issue at stake

The paper provides exact analytical results about the equilibrium pair correlation in a fluid of charged spheres in the vicinity of an insulating wall. The first motivation for the work was to cast the lightening of statistical mechanics of charge fluids on experiments that reported attractions between like-charge colloids in confined geometries. These colloids are mesoscopic spheres whose individual motion can be tracked with a conventional microscope and a video camera. Hence, the static pair distribution function $1+h_{\mathrm{col\,col}}(\mathbf{r},\mathbf{r}')$ between two colloidal spheres located at positions $\mathbf{r}$ and $\mathbf{r}'$, respectively, can be experimentally assessed when colloids are constrained to move in a given plane. [The static correlation $h_{\mathrm{col\,col}}(\mathbf{r},\mathbf{r}')$ is also known as the Ursell function; see e.g., Ref. [1].] The quantity of interest in experiments was the effective pairwise interaction $w_{\mathrm{col\,col}}(\mathbf{r},\mathbf{r}')$, also called potential of mean force. Quite generally, the effective interaction $w_{\alpha\alpha'}$ between two charges of species α and α' is defined from the Ursell function $h_{\alpha\alpha'}$ by

$$1+h_{\alpha\alpha'}\equiv\exp(-\beta w_{\alpha\alpha'}). \tag{1}$$

When species α has a packing fraction so high that the nearest-neighbor distance a_α is of the order of the range σ_α of short-ranged repulsions, $w_{\alpha\alpha}$ and $h_{\alpha\alpha}$ have oscillations with period a_α over a scale equal to a few a_α's [1]. When species α is very dilute, the oscillatory excluded-volume effect disappears, and, if other species have not far larger hard-core sizes, the functional forms of $w_{\alpha\alpha}$ and $h_{\alpha\alpha}$ at distances larger than σ_α are controlled by long-ranged pairwise interactions. For the considered colloids, which acquire a surface charge by solvatation, the long-range interaction is of electrostatic origin.

In an experiment carried in 1997 with dilute colloids in the vicinity of a glass wall [2], Larsen and Grier showed that $w_{\mathrm{col\,col}}$ for two colloids at the same distance x from the wall becomes attractive at large relative distances y. This result raised a debate (see Sec. VI A for more details) where all theoretical works predicted that there was no attraction at equilibrium. Eventually Squires and Brenner [3] argued that the attraction determined in Ref. [2] could be accounted for by an electrohydrodynamical effect linked to the electrostatic repulsion of colloids from the surface charge of the wall (which has the same sign as that of colloids). However, at-

*Present address: Institute for Physical Science and Technology, University of Maryland, College Park, Maryland 20910, USA.

†Laboratoire associé au Center National de la Recherche Scientifique, UMR 5672.

‡Laboratoire associé au Center National de la Recherche Scientifique, UMR 8627.

traction between like-charge colloids has also been observed in several experiments where suspensions are confined between two plates (see references quoted in Ref. [4]). In the latest one [4], Han and Grier still find an attraction, though kinematic effects are negligible. Therefore, a question remains open: at equilibrium might confinement combined with many-body effects induce an effective attraction between like charges at large relative distances?

The aim of the present paper is to revisit the structure of the large-distance behavior of the equilibrium correlation between dilute colloids in the vicinity of a single glass wall, thanks to exact results derived in the framework of statistical mechanics of charged fluids. We consider a fluid of charged spheres at equilibrium in the vicinity of an insulating wall characterized by its dielectric constant ϵ_W. Microscopic pair interactions are sums of purely charge-charge Coulomb forces and hard-core repulsions. Coulomb interaction between two charges e_α and $e_{\alpha'}$ of species α and α' located at positions $\mathbf{r}$ and $\mathbf{r}'$, respectively, is written as $(e_\alpha e_{\alpha'}/\epsilon_{\rm solv})v(\mathbf{r},\mathbf{r}')$, where $\epsilon_{\rm solv}$ is the solvent dielectric constant and $v(\mathbf{r},\mathbf{r}')$ is the solution of the Poisson equation with adequate boundary conditions. For point charges, the Poisson equation in the Gauss units reads

$$\Delta_{\mathbf{r}} v(\mathbf{r},\mathbf{r}') = -4\pi\delta(\mathbf{r}-\mathbf{r}'). \tag{2}$$

For charges spread over spheres, the Dirac distribution $\delta(\mathbf{r}-\mathbf{r}')$ is to be replaced by a surface distribution. In the vicinity of a wall, symmetries enforce that $h_{\alpha\alpha'}(\mathbf{r},\mathbf{r}') = h_{\alpha\alpha'}(x,x',y)$, where x and x' are the distances of $\mathbf{r}$ and $\mathbf{r}'$ from the wall, while y is the norm of the projection of $\mathbf{r}-\mathbf{r}'$ onto the wall plane.

It is well known that, far away from the wall, correlations decay exponentially fast when the distance between charges goes to infinity. On the contrary, in the vicinity of a wall, deformations of screening clouds enforced by the presence of the wall is expected to generate algebraic effective interactions between charges (see Ref. [5] for a review). At sufficiently large distances y along the wall, the $1/y^3$ interactions dominate all other tails, which decay either algebraically or exponentially,

$$h_{\alpha\alpha'}(x,x',y) \underset{y\to+\infty}{\sim} -\beta\frac{f_{\alpha\alpha'}(x,x')}{y^3}, \tag{3}$$

where $\beta = 1/k_{\rm B}T$ is the inverse temperature. ($k_{\rm B}$ is the Boltzmann constant and T is the absolute temperature.) On one hand, property (3) can be inferred from explicit calculations in the weak-coupling limit [6–8]. On the other hand, the existence of the $1/y^3$ decay is confirmed by a mesoscopic result. By an argument based on linear response theory and macroscopic electrostatics, Jancovici [9] settled that the correlation between the densities of global surface charges separated by a distance y decays as $1/y^3$ with a universal negative coefficient. The property can be written as

$$\int_0^{+\infty} dx \int_0^{+\infty} dx' \sum_{\alpha\alpha'} e_\alpha \rho_\alpha(x) e_{\alpha'} \rho_{\alpha'}(x') f_{\alpha\alpha'}(x,x') = \frac{(\epsilon_W/\epsilon_{\rm solv})}{8\pi^2\beta^2} \tag{4}$$

and the corresponding interaction is repulsive. Indeed, property (3) and relation (1) between $h_{\alpha\alpha'}$ and $w_{\alpha\alpha'}$ imply that in a dilute fluid

$$w_{\alpha\alpha'}(x,x',y) \underset{y\to+\infty}{\sim} \frac{f_{\alpha\alpha'}(x,x')}{y^3}. \tag{5}$$

We notice that the limit $y\to+\infty$ means that y is larger than the radii of particles, the screening length and the distance $y_\star(x,x')$ where exponential tails are overcome by the $1/y^3$ tail.

B. Main results

The structure of the function $f_{\alpha\alpha'}(x,x')$ is investigated for any value of the Coulomb coupling in the dilute fluid phase. The main results of our analysis and their consequences in the case of dilute colloid suspensions are the following.

First, the immersion free energy u_{qq} of two external charges q in a dilute electrolytic solution has a $1/y^3$ tail, which is *repulsive* for any x or x' when it is calculated in a linearized mean-field scheme. When the electrolyte is dilute, the large-distance behavior of $u_{qq} = (q^2/\epsilon_{\rm solv})\psi$ can be calculated by a mean-field theory, because of the long range of the Coulomb interaction. Moreover, if the Coulomb coupling is weak at considered distances or if q is infinitesimal, a linearization in q can be performed. In a linearized mean-field approximation [10] ψ^{LMF} is independent of q and coincides with the screened potential ϕ that arises in the formalism devised in Sec. II. In Sec. III we show that, at large distances y along the wall, $\phi(x,x',y)$ has a $1/y^3$ tail with a positive coefficient at all distances x and x' from the wall

$$\phi(x,x',y) \underset{y\to+\infty}{\sim} \frac{f_\phi(x,x')}{y^3} \quad \text{with} \quad f_\phi(x,x')>0. \tag{6}$$

In the case of a suspension of colloids with bare solvated charge $Z_{\rm col}e$ (where e denotes the absolute value of the electron charge), in the limit where colloids are infinitely diluted $w_{\rm col\,col}$ tends to the immersion free energy of an isolated pair $u_{\rm col\,col} = ([Z_{\rm col}e]^2/\epsilon_{\rm solv})\psi_{\rm ion}$, where $\psi_{\rm ion}$ is calculated in a fluid that does not contain any colloid. In a linearized mean-field approximation, $\psi^{LMF}_{\rm ion} = \phi_{\rm ion}$ and the free energy $u^{LMF}_{\rm col\,col}$ has a repulsive tail by virtue of Eq. (6). Besides, in a colloidal suspension at finite dilution, the linearized mean-field approximation $w^{LMF}_{\rm col\,col}$ for the effective interaction between colloids also has a repulsive $1/y^3$ tail. Indeed, $w^{LMF}_{\rm col\,col}$ is proportional to ϕ [6,11]: as for any species α, $w^{LMF}_{\rm col\,col} = -h^{LMF}_{\rm col\,col}/\beta = ([Z_{\rm col}e]^2/\epsilon_{\rm solv})\phi$, where ϕ is calculated in a fluid that contains colloids.

Second, the coefficient $f_\phi(x,x')$ of the $1/y^3$ tail of $\phi(x,x',y)$ is shown to take a dipolar form when both x and x' are larger than $b_{\max}$, the biggest one among the closest approach distances b_α's to the wall for every species α,

$$f_\phi(x,x')=\bar{D}_\phi(x)\bar{D}_\phi(x') \quad (7)$$

$$\text{when } x>b_{\max} \text{ and } x'>b_{\max}.$$

The effective dipole $\bar{D}_\phi(x)$ has a constant sign when x varies from $b_{\max}$ to $+\infty$.

If all species have the same closest approach distance b to the wall—as it is the case in an electrolyte where the differences in the various ion diameters are negligible with respect to all other characteristic lengths—Eq. (7) implies that $\phi(x,x',y)$ has the dipolar structure $\bar{D}_\phi(x)\bar{D}_\phi(x')/y^3$ at all distances x and x' in the fluid. Then, as shown in Sec. IV, $f_{\alpha\alpha'}(x,x')$ defined in Eq. (3) is, in fact, equal to the product

$$f_{\alpha\alpha'}(x,x';b)=D_\alpha(x)D_{\alpha'}(x') \quad (8)$$

$$\text{if } b_\alpha=b \text{ for all species.}$$

The function $D_\alpha(x)$ in Eq. (8) is to be interpreted as the dipole associated with a charge and its screening cloud. Its shape is a function of x more complicated than the mere exponential decay (74), with $A_\phi=1$, calculated in the weak-coupling and high-dilution limit. [The first correction to Eq. (74) is calculated in a forthcoming paper [12] for the primitive model defined hereafter when the wall carries no surface charge.] The sign of $D_\alpha(x)$ may vary with x.

Results (6)–(8) are valid for any strength of the Coulomb coupling in a dilute fluid phase and for species with various excluded-volume sizes. (The closest approach distance of a particle to the wall is not necessarily determined only by its size.) As discussed in Sec. V, these results also hold when the wall carries a surface charge, or when the charge of some species is not concentrated at a point, but spread on a sphere.

When all species have the same closest approach distance to the wall, an important consequence of factorization (8) of $f_{\alpha\alpha'}$ into a product of dipoles is that the effective interaction between like charges ($\alpha=\alpha'$) is repulsive when $x=x'$. On the contrary, when the species have different closest approach distances b_α's to the wall, as it is the case in a colloidal suspension, $f_{\alpha\alpha'}(x,x')$ is not factorized contrarily to Eq. (8) and $f_{\alpha\alpha}(x,x')$ for like charges may have any sign *a priori*, even when $x=x'$.

The behavior of electrostatic correlations in the experiment of Ref. [2] about dilute colloids is discussed in Sec. VI. The relevance of the present model is checked from the experimental data in the bulk. At investigated relative distances, electrostatic forces dominate short-range interactions and the functional form of the effective interaction is controled by the monopole-monopole part of electrostatic forces. The crossover from exponential to algebraic tails is numerically estimated. Comparison with experimental curves shows that the linearized mean-field scheme is relevant. We point out differences with the case where the colloidal suspension is confined between two plates.

The latter discussion is postponed to Sec. VI, since it is performed in the lightning of the exact results about $h_{\alpha\alpha'}$ that are derived through Secs. II to V. However, Sec. VI is written in a rather self-contained way and the reader not interested in formalism developments may skip Secs. II to V.

C. Methods

Before going into details, we summarize the general method displayed in Secs. II–IV. The Ursell function $h_{\alpha\alpha'}$ for the so-called primitive model (Sec. II A), in the bulk as well as near the wall, is studied from the Mayer diagrammatics (Sec. II B). (In the Mayer diagrams, the difference between both situations is just that, in the second case, species densities depend on the distance x from the wall.) Integrals corresponding to the Mayer diagrams diverge, because of the long range of the Coulomb potential far away from the wall as well as in its vicinity. Then systematic resummations of long-ranged Coulomb divergences similar to that performed by Meeron for bulk quantities [13] provide diagrammatics where there appears a screened potential ϕ (Sec. II C). (Resummations rely on the same topological principles in both cases.) In the bulk, ϕ is a solution of the usual Debye equation. Near the wall ϕ obeys an ''inhomogeneous'' Debye equation (25), where the inverse screening length depends on x (Sec. II D). The large-distance behavior of $h_{\alpha\alpha'}$ can be conveniently studied by the new reorganization of diagrams that we introduce in Sec. II E. In Sec. III A we give the formal expression of the screened potential in the vicinity of the wall. (It has been determined in Ref. [14] in a simpler situation, namely, for an analogous screened potential that arises in a resummed fugacity Mayer expansion for the density when all closest approach distances b_α's are equal to the same value.) An analysis of the Fourier transform of ϕ shows that ϕ decays as $f_\phi(x,x')/y^3$ at large distances y with a constant sign (Sec. III B). Two sum rules for $\int d\mathbf{y}\phi(x,x',\mathbf{y})$ and $f_\phi(x,x')$, respectively, are settled in Sec. III C. These sum rules ensure that in the linearized mean-field approximation $h^{LMF}_{\alpha\alpha'}$ obeys the local electroneutrality sum rule (52) and sum rule (4). The sum rule satisfied by $f_\phi(x,x')$ allows one to derive its sign (6). In Sec. IV we show, thanks to the diagrammatic reorganization introduced in Sec. II E, that dipolar structure (7) of the $1/y^3$ tail of ϕ enforces that, when all species have the same closest approach distance to the wall, the coefficient of the $1/y^3$ tail in the correlation function $h_{\alpha\alpha'}$ takes form (8) for any value of the coupling parameter (temperature and bulk densities) in the fluid phase. Technical details are given in the Appendix.

II. GENERAL FORMALISM

A. Primitive model

Our system is a three-dimensional charge fluid confined to the region $x>0$ by a plane impenetrable dielectric wall, the electrostatic response of which is taken into account by a dielectric constant ϵ_W. Up to Sec. V A included, the solution is described by the usual *primitive model* [15] with n_s species of charges. In this model every charged particle of species α is represented as a hard sphere—with diameter σ_α—where the net charge $e_\alpha\equiv Z_\alpha e$ is concentrated at the center of the sphere. (We recall that e denotes the absolute value of the electron charge and Z_α may be negative.) The

extension of our results to the case where the charge of one species is uniformly spread on the surface of the hard-core sphere is discussed in Sec. V B. In the primitive model the solvent (water) is handled with as a continuous medium with a uniform dielectric constant $\epsilon_{\rm solv}$. Moreover, particles are assumed to be made of a material with the same dielectric constant as the solvent. Therefore, $\epsilon=\epsilon_{\rm solv}$ when $x>0$ and $\epsilon=\epsilon_{\rm W}$ when $x<0$.

Since a half space is occupied by a dielectric material, $v(\mathbf{r},\mathbf{r}')$ in the Coulomb pair interaction $(e_\alpha e_{\alpha'}/\epsilon_{\rm solv})v(\mathbf{r},\mathbf{r}')$ is solution of Poisson equation (2) with the adequate boundary conditions and it reads for $x>0$ and $x'>0$ [16]

$$v(\mathbf{r},\mathbf{r}')=\frac{1}{|\mathbf{r}-\mathbf{r}'|}-\Delta_{\rm el}\frac{1}{|\mathbf{r}-\mathbf{r}'^{\star}|} \tag{9}$$

with

$$\Delta_{\rm el}\equiv\frac{\epsilon_{\rm W}-\epsilon_{\rm solv}}{\epsilon_{\rm W}+\epsilon_{\rm solv}}. \tag{10}$$

In Eq. (9) $\mathbf{r}'^{\star}$ is the *image* of the position $\mathbf{r}'$ by the reflection with respect to the plane interface between the solution and the dielectric material. *A priori* $\Delta_{\rm el}$ ranges from -1 to 1. In the case of a glass wall in contact with water, $\epsilon_{\rm solv}\sim 80$, while ϵ_W is equal to a few units; then the relative dielectric constant $\epsilon_W/\epsilon_{\rm solv}$ of the wall with respect to the solvent is of order 1/80 and $\Delta_{\rm el}\sim -0.98$. In the bulk, far away from the wall, the expression of $v(\mathbf{r},\mathbf{r}')$ is reduced to $1/|\mathbf{r}-\mathbf{r}'|$. The hard-core interaction v_{SR} between two species α and α' is infinitely repulsive at distances shorter than the sum $(\sigma_\alpha+\sigma_{\alpha'})/2$ of the sphere radii of both species:

$$\beta v_{SR}(|\mathbf{r}-\mathbf{r}'|;\alpha,\alpha')=\begin{cases}+\infty, & \text{if } |\mathbf{r}-\mathbf{r}'|<(\sigma_\alpha+\sigma_{\alpha'})/2\\ 0, & \text{if } |\mathbf{r}-\mathbf{r}'|>(\sigma_\alpha+\sigma_{\alpha'})/2.\end{cases} \tag{11}$$

In fact, as discussed at the end of Sec. IV, the specific form of $v_{SR}(|\mathbf{r}-\mathbf{r}'|;\alpha,\alpha')$ has no consequence upon results (6)–(8). The expression (11) could be replaced by a more general soft short-ranged repulsion, the range of which would be of the order of $(\sigma_\alpha+\sigma_{\alpha'})/2$. In the primitive model defined just above, the total pair energy $U_{\rm pair}$ reads

$$U_{\rm pair}=\sum_{i<j} v_{SR}(|\mathbf{r}_i-\mathbf{r}_j|;\alpha_i,\alpha_j)+\frac{e^2}{\epsilon_{\rm solv}}\sum_{i<j} Z_{\alpha_i}Z_{\alpha_j}v(\mathbf{r}_i,\mathbf{r}_j), \tag{12}$$

where i is the index of a particle.

In the vicinity of the wall, one-body potentials appear in the total energy of the system. For every charge a self-energy $Z_\alpha^2(e^2/\epsilon_{\rm solv})V_{\rm self}(x)$ arises from the work necessary to bring a charge $Z_\alpha e$ from $x=+\infty$ (in the solvent) to a point $\mathbf{r}$ in the vicinity of the wall. According to Eq. (9), the wall electrostatic response is equivalent to the presence of an image charge $-\Delta_{\rm el}Z_\alpha(e/\sqrt{\epsilon_{\rm solv}})$ at point $\mathbf{r}^{\star}$, and

$$V_{\rm self}(x)=-\Delta_{\rm el}\frac{1}{4x}. \tag{13}$$

As mentioned above, when the solvent is water and the wall is made of glass, $\Delta_{\rm el}$ defined in Eq. (10) is negative, and $V_{\rm self}(x)$ is a repulsive potential. The impenetrability of the wall corresponds to a short-ranged potential

$$\beta V_{SR}(x;\alpha)=\begin{cases}+\infty, & \text{if } x<b_\alpha\\ 0, & \text{if } x>b_\alpha,\end{cases} \tag{14}$$

where b_α is the closest approach distance of the center of a particle α to the wall. The confinement of all particles to the positive-x region and the electrostatic self-energy may be gathered into a one-body potential $V_{\rm wall}$:

$$V_{\rm wall}=\sum_i V_{SR}(x_i;\alpha_i)+\frac{e^2}{\epsilon_{\rm solv}}\sum_i Z_{\alpha_i}^2 V_{\rm self}(x_i). \tag{15}$$

B. Generalized Mayer diagrams

The system at equilibrium at inverse temperature β in a finite volume Λ can be studied in the grand canonical ensemble where each species α has a fixed fugacity z_α. The grand canonical function Ξ is defined by

$$\Xi(\beta,\{z_\alpha\}_{\alpha=1,\ldots,n_s},\Lambda)=\sum_{\{N_\alpha\}_{\alpha=1,\ldots,n_s}}\left[\prod_\alpha\frac{z_\alpha^{N_\alpha}}{N_\alpha!}\right]\int_\Lambda\left[\prod_{i=1}^{\Sigma_\alpha N_\alpha}d\mathbf{r}_i\right]\times e^{-\beta[U_{\rm pair}+V_{\rm wall}]}. \tag{16}$$

In Eq. (16) N_α is the total number of particles with species α and $\Sigma_{\{N_\alpha\}_{\alpha=1,\ldots,n_s}}$ denotes the summation over all possible combinations of n_s N_α's. Near the wall, Λ denotes a finite-size region bounded by the wall on the left. In the bulk, Λ stands for a finite-size region far away from the wall, $v(\mathbf{r},\mathbf{r}')$ is reduced to its bulk value and $V_{\rm wall}$ does not appear in Eq. (16).

In order to write a single formula for Ξ, whether Λ lies near the wall or in the bulk, we introduce a generalized fugacity that incorporates the one-body potential created by the wall, as we have already done in Ref. [14]. The generalized fugacity $\bar{z}_\alpha(x)$ depends only on the distance x to the wall, and reads

$$\bar{z}_\alpha(x)=z_\alpha\exp\left[-\beta V_{SR}(x;\alpha)-\frac{\beta e^2}{\epsilon_{\rm solv}}Z_\alpha^2 V_{\rm self}(x)\right]. \tag{17}$$

Moreover, the summation over the N_α's can be replaced by a summation over $N=\Sigma_\alpha N_\alpha$ with the result

$$\Xi(\beta,\{z_\alpha\}_{\alpha=1,\ldots n_s},\Lambda)=\sum_{N=0}^{+\infty}\frac{1}{N!}\int_\Lambda\left[\prod_{n=1}^{N}d\mathbf{r}_n\left(\sum_{\alpha_n=1}^{n_s}\bar{z}_{\alpha_n}(x_n)\right)\right]e^{-\beta U_{\rm pair}}. \tag{18}$$

We use the convention that when $N=0$ the integral is reduced to 1. Then the fugacity expansion of the density pro-

file $\rho_\alpha(x)$ can be represented by the generalized Mayer diagrams where each pair of points labeled by n and m is linked by at most one bond

$$f(n,m)=\exp\left[-\beta\left(v_{SR}(|\mathbf{r}_n-\mathbf{r}_m|;\alpha_n,\alpha_m)+\frac{e^2}{\epsilon_{\rm solv}}Z_{\alpha_n}Z_{\alpha_m}v(\mathbf{r}_n,\mathbf{r}_m)\right)\right]-1. \tag{19}$$

In the integral associated with every diagram, each point has an x-dependent weight $\bar{z}_\alpha(x)$, which is summed over all species. Because of the long range of the Coulomb potential, every integral corresponding to a Mayer diagram that is not sufficiently connected diverges when the volume Λ becomes infinite—inside the bulk or on the right of the wall—but systematic resummations remove these divergences (see Ref. [14]).

The density expansion of $h_{\alpha\alpha'}$ can also be expressed in terms of the Mayer diagrams with bonds (19) (see, e.g., Ref. [1] for the homogeneous case). The general formula, where uniform densities are replaced by density profiles in the present case, is

$$h_{\alpha\alpha'}(x,x',\mathbf{y})=\sum_\Gamma \frac{1}{S_\Gamma}\int_\Lambda\left[\prod_{n=1}^{N} d\mathbf{r}_n\left(\sum_{\alpha_n=1}^{n_s}\rho_{\alpha_n}(x_n)\right)\right]\times\left[\prod f\right]_\Gamma. \tag{20}$$

In Eq. (20) the sum runs over all unlabeled topologically different connected diagrams Γ with two root points $(\mathbf{r},\alpha)$ and $(\mathbf{r}',\alpha')$ (which are not integrated over) and N internal points (which are integrated over) with $N=0,\ldots,\infty$. A diagram Γ is built according to the following rules. Each pair of points in Γ is linked by at most one f bond, there is no articulation point and every internal point has a weight equal to $\Sigma_{\alpha_n=1}^{n_s}\rho_{\alpha_n}(x_n)$. (An articulation point is defined by the fact that, if it is taken out of the diagram, then the diagram is split into two pieces, one of which at least is no longer linked to any root point.) $[\Pi f]_\Gamma$ is the product of the f bonds in the Γ diagram and S_Γ is its symmetry factor, i.e., the number of permutations of the internal points $\mathbf{r}_n$ that do not change this product. We have used the convention that, if N is equal to 0, no $\int d\mathbf{r}_n[\Sigma_{\alpha_n=1}^{n_s}\rho_{\alpha_n}(x_n)]$ appears and $(1/S_\Gamma)[\Pi f]_\Gamma$ is reduced to $f(\mathbf{r},\mathbf{r}')$. Similar to what happens for the Mayer diagrammatic representations of fugacity expansions for density profiles, integrals in Eq. (20) diverge in the infinite volume limit, because of the long range of the Coulomb interaction. Then systematic partial resummations must be performed, as shown in the following subsection.

C. Systematic resummations of Coulomb divergences

The method that we use is a generalization of the procedure introduced by Meeron [13] to calculate $h_{\alpha\alpha'}$ in the bulk; the only difference is that point weights in the Mayer diagrams are now x dependent. The starting trick is to split the Mayer bond (19) into two auxiliary bonds: the "Coulomb" bond $f^{\rm cc}\equiv-\beta e^2 Z_{\alpha_n}Z_{\alpha_m}v(\mathbf{r}_n,\mathbf{r}_m)$ and its complementary function $f-f^{\rm cc}$. Then subdiagrams containing chains of the Coulomb bonds $f^{\rm cc}$ are resummed inside equivalence classes. The potential ϕ, which arises as the sum of chains with all possible lengths made with $f^{\rm cc}$ bonds, can be viewed as the solution of the integral equation

$$\phi(\mathbf{r},\mathbf{r}')=v(\mathbf{r},\mathbf{r}')-\frac{\beta e^2}{\epsilon_{\rm solv}}\int_\Lambda d\mathbf{r}''\sum_{\alpha=1}^{n_s}Z_\alpha^2\rho_\alpha(x'')v(\mathbf{r},\mathbf{r}'')\phi(\mathbf{r}'',\mathbf{r}'), \tag{21}$$

$\phi(\mathbf{r},\mathbf{r}')$ is also the solution of another integral equation, which is obtained from Eq. (21) by exchanging the roles of $\mathbf{r}$ and $\mathbf{r}'$. Equation (21) coincides with the equation obeyed by a linearized mean-field approximation for the immersion free energy of two external charges [10]. It also coincides with the equation obeyed by the linearized mean-field Ursell function $-\beta(e^2/\epsilon_{\rm solv})Z_\alpha Z_{\alpha'}\phi$ [6,11].

Topological considerations used by Meeron (and reformulated in Refs. [17] for bulk correlations in quantum Coulomb fluids) lead to the following resummed diagrammatic representation of $h_{\alpha\alpha'}$,

$$h_{\alpha\alpha'}(x,x',\mathbf{y})=\sum_\Pi \frac{1}{S_\Pi}\int_\Lambda\left[\prod_{n=1}^{N} d\mathbf{r}_n\left(\sum_{\alpha_n=1}^{n_s}\rho_{\alpha_n}(x_n)\right)\right]\times\left[\prod F\right]_\Pi. \tag{22}$$

Diagrams Π are defined as diagrams Γ in the initial diagrammatic representation (20) with only two differences. First, the bond f is replaced by two resummed bonds F called $F^{\rm cc}$ and $F_{\rm R}$ with

$$F^{\rm cc}(n,m)=-\frac{\beta e^2}{\epsilon_{\rm solv}}Z_{\alpha_n}Z_{\alpha_m}\phi(\mathbf{r}_n,\mathbf{r}_m) \tag{23}$$

and

$$F_{\rm R}(n,m)=\exp\left[-\beta\left(v_{SR}(|\mathbf{r}_n-\mathbf{r}_m|;\alpha_n,\alpha_m)+\frac{e^2}{\epsilon_{\rm solv}}Z_{\alpha_n}Z_{\alpha_m}\phi(\mathbf{r}_n,\mathbf{r}_m)\right)\right]-1+\frac{\beta e^2}{\epsilon_{\rm solv}}Z_{\alpha_n}Z_{\alpha_m}\phi(\mathbf{r}_n,\mathbf{r}_m). \tag{24}$$

Second, in order to avoid double counting in the resummation process, diagrams Π must be built with an "excluded-composition" rule: there is no point linked to the rest of the diagram by only two $F^{\rm cc}$ bonds. As can be checked from the properties derived in Sec. III, the screened potential ϕ is integrable at large distances and Π diagrams correspond to convergent integrals in the limit where the volume Λ extends to infinity inside the bulk or on the right of the wall.

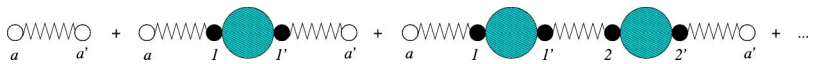

FIG. 1. Representation of $h^{cc}_{\alpha\alpha'}(\mathbf{r},\mathbf{r}')$ as the graph series defined in Eq. (31). A wavy line represents a bond F^{cc} and a gray disk stands for a bond I. A couple of variables $(\mathbf{r}_i,\gamma_i)$ are associated with every circle. For a white circle $a=(\mathbf{r},\alpha)$ [or $a'=(\mathbf{r}',\alpha')$], $\mathbf{r}$ and α are fixed, whereas, for a black circle $i=(\mathbf{r}_i,\gamma_i)$, $\mathbf{r}_i$ and γ_i are integrated with the measure $\int d\mathbf{r}_i \Sigma_{\alpha_i}\rho_{\alpha_i}(\mathbf{r}_i)$.

D. Screened potential

Since Coulomb potential $v(\mathbf{r},\mathbf{r}')$ for point charges is a solution of Poisson equation (2), integral equation (21) which defines the screened potential ϕ can be turned into the partial derivative equation

$$\Delta_{\mathbf{r}}\phi(\mathbf{r},\mathbf{r}')-\bar{\kappa}^2(x)\phi(\mathbf{r},\mathbf{r}')=-4\pi\delta(\mathbf{r}-\mathbf{r}'), \tag{25}$$

where $\bar{\kappa}^2(x)$ is defined as

$$\bar{\kappa}^2(x)\equiv 4\pi\beta\frac{e^2}{\epsilon_{\text{solv}}}\sum_{\alpha} Z_\alpha^2\rho_\alpha(x). \tag{26}$$

The presence of the hard-core repulsion (14) from the wall enforces that $\rho_\alpha(x)$ vanishes for $x<b_\alpha$. Since ϕ arises as the infinite sum of the Coulomb chains defined in Sec. II C, ϕ obeys the same boundary conditions as Coulomb potential v. $\phi(\mathbf{r},\mathbf{r}')$ tends to 0 when $|\mathbf{r}-\mathbf{r}'|$ goes to $+\infty$, it is continuous everywhere while its normal gradient times the dielectric constant is continuous at the interface with dielectric walls. We recall that particles are supposed to be made of a material with the same dielectric constant as the solvent.

In the bulk, far away from any boundary, $\bar{\kappa}(x)$ becomes a constant equal to the inverse Debye screening length κ_D:

$$\kappa_D=\sqrt{\frac{4\pi\beta e^2}{\epsilon_{\text{solv}}}\sum_{\alpha} Z_\alpha^2\rho_\alpha^{\text{B}}}, \tag{27}$$

where ρ_α^{B} is the bulk density of species α. Then Eq. (25) is the usual Debye equation. Since ϕ in the bulk is a function of $|\mathbf{r}-\mathbf{r}'|$ that vanishes when $|\mathbf{r}-\mathbf{r}'|$ goes to infinity, it is equal to the well-known Debye potential

$$\phi^{\text{D}}(|\mathbf{r}-\mathbf{r}'|)=\frac{e^{-\kappa_D|\mathbf{r}-\mathbf{r}'|}}{|\mathbf{r}-\mathbf{r}'|}. \tag{28}$$

Near the plane dielectric wall located at $x=0$, Eq. (25) is an "inhomogeneous" Debye equation, where the inverse squared screening length $\bar{\kappa}^2$ depends on the distance x from the wall. The function $\bar{\kappa}^2(x)$ has finite steps at points $x=b_\alpha$ with $\alpha=1,\ldots,n_s$. $\phi(\mathbf{r},\mathbf{r}')$ is continuous everywhere and obeys the boundary condition

$$\lim_{x\to 0^-}\frac{\epsilon_{\text{W}}}{\epsilon_{\text{solv}}}\frac{\partial\phi}{\partial x}(\mathbf{r},\mathbf{r}')=\lim_{x\to 0^+}\frac{\partial\phi}{\partial x}(\mathbf{r},\mathbf{r}'), \tag{29}$$

where $x'\neq 0$. $\partial\phi/\partial x(\mathbf{r},\mathbf{r}')$ is continuous at every b_α when $\mathbf{r}\neq\mathbf{r}'$.

E. Reorganization of resummed diagrammatics

In the absence of any compensation mechanism, the Ursell function $h_{\alpha\alpha'}$ is expected to decay at large distances as the slowest bond in its resummed diagrammatic representation (22), namely, as F^{cc}. [F_{R} falls off as the squared tail of F^{cc} by virtue of (23) and (24).] In order to analyze the large-distance behavior of $h_{\alpha\alpha'}$, we proceed to the following diagrammatic reorganization.

In a first step, we reorganize the resummed Mayer diagrammatics (22) for $h_{\alpha\alpha'}$ into a sum of graphs built with the bond F^{cc} and with the bond I defined as the sum of all subdiagrams that either contain no F^{cc} bond or remain connected in a single piece when anyone among its F^{cc} bonds is cut. (In the following, we use the word "graph" for an object built with F^{cc} and I bonds, and we keep the term "diagram" for a resummed Mayer diagram made of F^{cc} and F_{R} bonds.) Since the reorganization is purely topological, it is valid for correlations in the bulk as well as in the vicinity of the wall.

The reason for this first reorganization is that the topology of subdiagrams involved in I has the following consequence. If F^{cc} decays algebraically in some direction, F_{R} decreases as the square of the decay law of F^{cc} in the same direction, and so does I. (A similar property has already been used in Refs. [18] and [19] for the investigation of algebraic decays in quantum bulk correlations.) If F^{cc} falls off exponentially fast at large distances $|\mathbf{r}-\mathbf{r}'|$, then I decays faster than F^{cc} at least in weak-coupling and high-dilution regimes. (The latter case will be investigated in detail in a forthcoming paper [12].)

In a second step, four classes of graphs in this new representation of $h_{\alpha\alpha'}(\mathbf{r}_a,\mathbf{r}_{a'})$ are distinguished by considering whether a single bond F^{cc} is attached either to root point $(\mathbf{r}_a,\alpha)$ or to root point $(\mathbf{r}_{a'},\alpha')$. According to the excluded-composition rule obeyed by resummed Π diagrams, $h_{\alpha\alpha'}$ can be rewritten as the sum

$$h_{\alpha\alpha'}\equiv h^{cc}_{\alpha\alpha'}+h^{c-}_{\alpha\alpha'}+h^{-c}_{\alpha\alpha'}+h^{--}_{\alpha\alpha'}, \tag{30}$$

where the functions on the right hand side of Eq. (30) are equal to the graph series represented in Figs. 1–3 respectively. [In the following a (a') is a short notation for the couple of variables $(\mathbf{r},\alpha)$ [$(\mathbf{r}',\alpha')$] associated with a root point, c represents $(\mathbf{r}_c,\gamma)$, and i stands for $(\mathbf{r}_i,\alpha_i)$.] The analytical definitions of the series are

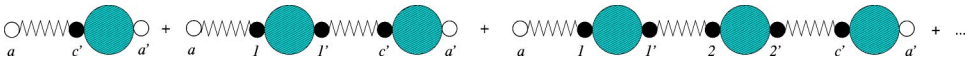

FIG. 2. Graphic representation of definition (32) for $h^{c-}_{\alpha\alpha'}(\mathbf{r},\mathbf{r}')$.

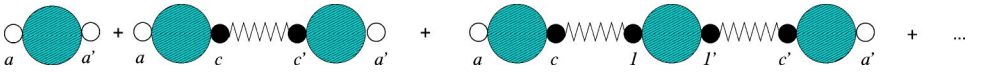

FIG. 3. Graphic representation of definition (33) for $h^{--}_{\alpha\alpha'}(\mathbf{r},\mathbf{r}')$.

$$h^{cc}_{\alpha\alpha'}(\mathbf{r},\mathbf{r}') \equiv F^{cc}(a,a') + \int d\mathbf{r}_1 d\mathbf{r}'_1 \sum_{\gamma_1,\gamma'_1} \rho_{\gamma_1}(\mathbf{r}_1)\rho_{\gamma'_1}(\mathbf{r}'_1) \times F^{cc}(a,1) I(1,1') F^{cc}(1',a') + \int d\mathbf{r}_1 d\mathbf{r}'_1 \sum_{\gamma_1,\gamma'_1} \rho_{\gamma_1}(\mathbf{r}_1)\rho_{\gamma'_1}(\mathbf{r}'_1) \times \int d\mathbf{r}_2 d\mathbf{r}'_2 \sum_{\gamma_2,\gamma'_2} \rho_{\gamma_2}(\mathbf{r}_2)\rho_{\gamma'_2}(\mathbf{r}'_2) \times F^{cc}(a,1) I(1,1') F^{cc}(1',2) I(2,2') F^{cc}(2',a') + \cdots, \tag{31}$$

$$h^{c-}_{\alpha\alpha'}(\mathbf{r},\mathbf{r}') \equiv \int d\mathbf{r}_{c'} \sum_{\gamma'} \rho_{\gamma'}(\mathbf{r}_{c'}) F^{cc}(a,c') I(c',a') + \int d\mathbf{r}_{c'} \sum_{\gamma'} \rho_{\gamma'}(\mathbf{r}_{c'}) \int d\mathbf{r}_1 d\mathbf{r}'_1 \sum_{\gamma_1,\gamma'_1} \rho_{\gamma_1}(\mathbf{r}_1) \times \rho_{\gamma'_1}(\mathbf{r}'_1) F^{cc}(a,1) I(1,1') F^{cc}(1',c') I(c',a') + \cdots, \tag{32}$$

while h^{-c} is defined in a symmetric way, and

$$h^{--}_{\alpha\alpha'}(\mathbf{r},\mathbf{r}') \equiv I(a,a') + \int d\mathbf{r}_c \int d\mathbf{r}_{c'} \sum_{\gamma,\gamma'} \rho_{\gamma}(\mathbf{r}_c)\rho_{\gamma'}(\mathbf{r}_{c'}) I(a,c) \times F^{cc}(c,c') I(c',a') + \int d\mathbf{r}_c \int d\mathbf{r}_{c'} \sum_{\gamma,\gamma'} \rho_{\gamma}(\mathbf{r}_c)\rho_{\gamma'}(\mathbf{r}_{c'}) \times \int d\mathbf{r}_1 d\mathbf{r}'_1 \sum_{\gamma_1,\gamma'_1} \rho_{\gamma_1}(\mathbf{r}_1)\rho_{\gamma'_1}(\mathbf{r}'_1) I(a,c) \times F^{cc}(c,1) I(1,1') F^{cc}(1',c') I(c',a') + \cdots. \tag{33}$$

We notice that I is the analog of the so-called single-particle irreducible function in the Feynman diagrammatics for the two-point propagator of an equivalent field theory (see, e.g., Ref. [20]).

III. PROPERTIES OF THE SCREENED POTENTIAL

In order to take advantage of the invariance along the directions parallel to the wall, we introduce the Fourier transform with respect to the $\mathbf{y}$ variable, and we write

$$\phi(x,x',\mathbf{y}) = \int \frac{d^2\mathbf{k}}{(2\pi)^2} e^{-i\mathbf{k}\cdot\mathbf{y}} \phi(x,x',\mathbf{k}). \tag{34}$$

After Fourier transformation (25) becomes the linear differential equation

$$\left\{ \frac{\partial^2}{\partial x^2} - \mathbf{k}^2 - \bar{\kappa}^2(x) \right\} \phi(x,x',\mathbf{k}) = -4\pi\delta(x-x'). \tag{35}$$

In the following, we assume that the species are labeled in such a way that $b_{\min} = b_1 < b_2 < \cdots < b_{n_s} = b_{\max}$. $\bar{\kappa}^2(x)$ and its first derivative are continuous in each interval $b_i < x < b_{i+1}$ (with the convention $b_{n_s+1} = +\infty$) and have only finite steps at every b_i.

A. Formal expression of ϕ

The explicit resolution of the inhomogeneous Debye equation (35) requires one to distinguish several regions. For our discussion we need to consider only four regions: region I for $x<0$, region II for $0<x<b_{\min}$, region III for $b_{\min}<x<b_{\max}$, and region IV for $b_{\max}<x$. The results summarized in the present subsection are a generalization of those derived in more detail for a similar but simpler equation in Ref. [14].

In the above regions I and II, $\bar{\kappa}^2(x)$ vanishes by virtue of Eq. (26). When $x' > b_{\min}$ Eq. (35) reads

$$\left\{ \frac{\partial^2}{\partial x^2} - \mathbf{k}^2 \right\} \phi(x,x',\mathbf{k}) = 0 \quad \text{if} \quad x < b_{\min}. \tag{36}$$

The solution with boundary conditions recalled after Eq. (26) [in particular, condition (29)] is

$$\phi(x,x',\mathbf{k}) = A(x',|\mathbf{k}|)(1-\Delta_{el}) e^{|\mathbf{k}|x} \quad \text{if} \quad x<0 (x'>b_{\min}) \tag{37}$$

and

$$\phi(x,x',\mathbf{k}) = A(x',|\mathbf{k}|)[e^{|\mathbf{k}|x} - \Delta_{el} e^{-|\mathbf{k}|x}] \quad \text{if} \quad 0<x<b_{\min} \ (x'>b_{\min}). \tag{38}$$

[In Ref. [14] there is a sign misprint in Eq. (4.20), which has to coincide with Eq. (38).]

When both $x > b_{\min}$ and $x' > b_{\min}$, $\delta(x-x')$ does not vanish for every x. The explicit solution for $\phi(x,x',\mathbf{k})$ is obtained by distinguishing the subregions separated by the planes $x = b_i$. Let us call (i) the subregion $b_i < x < b_{i+1}$ (with $b_{n_s+1} \equiv +\infty$). When x varies in subregion (i), $h_{(i)}$ denotes the continuous solution of the "homogeneous" equation associated with equation (35)—namely, the equation without the Dirac distribution term—and extended to the range $-\infty < x < +\infty$,

$$\left\{\frac{\partial^2}{\partial x^2}-\mathbf{k}^2-\bar{\kappa}^2(x)\right\}h_{(i)}(x,\mathbf{k}^2)=0. \tag{39}$$

In Eq. (39) only species $\alpha=1,\ldots,i$ do contribute to $\bar{\kappa}^2(x)$ defined in Eq. (26). The general solution of Eq. (35) for x in subregion (i) and x' in subregion (i') is the sum of a linear combination of two independent solutions $h^+_{(i)}$ and $h^-_{(i)}$ plus, if $(i)=(i')$, a particular solution $\phi_{\mathrm{sing}(i)}$ of Eq. (35), which is singular when $x=x'$ and which is calculated in terms of $h^+_{(i)}$ and $h^-_{(i)}$ by the so-called Wronskian method [21]. In the following, $h^+_{(i)}$ ($h^-_{(i)}$) is chosen to be a solution that vanishes (diverges) when x tends to $+\infty$. (In the bulk, $\bar{\kappa}(x)$ is a constant equal to the inverse Debye length κ_D: h^+ and h^- can be chosen to be equal to $\exp[\mp x\sqrt{\kappa_D^2+\mathbf{k}^2}]$.) Since $\phi(x,x',\mathbf{k})$ also obeys a second equation given by Eq. (35) where the roles of x and x' are exchanged [see the comment after Eq. (21)], $\phi(x,x',\mathbf{k})$ for x in subregion (i) and for x' in subregion (i') is equal to

$$\begin{aligned}\phi(x,x',\mathbf{k})=&\,\delta_{i,i'}\phi_{\mathrm{sing}(i)}(x,x',\mathbf{k}^2)\\&+\sum_{\varepsilon=+,-}\sum_{\varepsilon'=+,-}Z^{\varepsilon\varepsilon'}_{(ii')}(|\mathbf{k}|)\\&\times h^{\varepsilon}_{(i)}(x,\mathbf{k}^2)h^{\varepsilon'}_{(i')}(x',\mathbf{k}^2).\end{aligned} \tag{40}$$

The coefficients $Z^{\pm\pm}_{(ii')}$ are determined by the continuity of $\phi(x,x',\mathbf{k})$ at the planes $x=b_1,\ldots,b_{n_s}$ and $x'=b_1,\ldots,b_{n_s}$, the continuity of $\partial\phi(x,x',\mathbf{k})/\partial x$ and $\partial\phi(x,x',\mathbf{k})/\partial x'$ at the same planes, and the vanishing of $\phi(x,x',\mathbf{k})$ when x or x' goes to infinity. When both $x>b_{\max}$ and $x'>b_{\max}$, namely, when x and x' are in region IV, the vanishing of $\phi(x,x',\mathbf{k})$ at large distances x and x' enforces a simpler expression,

$$\begin{aligned}\phi_{IV}(x,x',\mathbf{k})=&\,\phi_{\mathrm{sing}IV}(x,x',\mathbf{k}^2)\\&+Z_{IV}(|\mathbf{k}|)h^+_{IV}(x,\mathbf{k}^2)h^+_{IV}(x',\mathbf{k}^2)\\&\text{if } x>b_{\max} \text{ and } x'>b_{\max}\end{aligned} \tag{41}$$

with

$$\begin{aligned}\phi_{\mathrm{sing}IV}(x,x',\mathbf{k}^2)=&-\frac{4\pi}{W_{IV}(\mathbf{k}^2)}h^-_{IV}(\inf(x,x'),\mathbf{k}^2)\\&\times h^+_{IV}(\sup(x,x'),\mathbf{k}^2),\end{aligned} \tag{42}$$

where $\inf(x,x')$ [$\sup(x,x')$] is the infimum (supremum) of x and x' and $W_{IV}(\mathbf{k}^2)$ is the Wronskian of solutions $h^+_{IV}(x,\mathbf{k}^2)$ and $h^-_{IV}(x,\mathbf{k}^2)$ defined as $W_{IV}(\mathbf{k}^2)=h^-_{IV}(\partial h^+_{IV}/\partial x)-h^+_{IV}(\partial h^-_{IV}/\partial x)$.

B. Small-k expansion of ϕ

The small-$\mathbf{k}$ expansions of $Z_{IV}(|\mathbf{k}|)$ and of the various other $Z^{\pm\pm}_{(ii')}(|\mathbf{k}|)$'s defined in Eq. (40) involve odd powers of $|\mathbf{k}|$, whereas other functions of $\mathbf{k}$ in ϕ proves to be functions of $\mathbf{k}^2$ [see Eq. (40)–(42)]. Indeed, $Z_{IV}(|\mathbf{k}|)$ and every $Z^{\pm\pm}_{(ii')}(|\mathbf{k}|)$ are determined by the ratio of the boundary equations obeyed by ϕ, $\partial\phi/\partial x$, and $\partial\phi/\partial x'$ at the various planes $x=b_i$ and $x'=b_{i'}$, while the x dependence of ϕ in regions I and II involves the functions $\exp(|\mathbf{k}|x)$ and $\exp(-|\mathbf{k}|x)$ [see Eqs. (37) and (38)].

We stress that the existence of odd powers of $|\mathbf{k}|$ in the small-$\mathbf{k}$ expansion of $\phi(x,x',\mathbf{k})$ is not specific to the particular form (14) of $V_{SR}(x;\alpha)$. It arises through the boundary conditions from the vanishing of the densities in region $x<0$ with a corresponding solution that takes the functional form (37).

Moreover, the coefficient $B^{[1]}_{Z_{IV}}$ of $|\mathbf{k}|$ in the small-$\mathbf{k}$ expansion of $Z_{IV}(|\mathbf{k}|)$ does not vanish when ϵ_W is finite,

$$Z_{IV}(|\mathbf{k}|)=Z_{IV}(\mathbf{k}=\mathbf{0})+|\mathbf{k}|B^{[1]}_{Z_{IV}}+O(\mathbf{k}^2), \tag{43}$$

and we expect that the same is true for every nonvanishing $Z^{\pm\pm}_{(ii')}(|\mathbf{k}|)$. [In Eq. (43) $\mathcal{O}(\mathbf{k}^2)$ denotes a term of order $\mathbf{k}^2$.] Property (43) can be checked from the expansions at the first two orders in the Coulomb coupling parameter in the case where all b_α's are equal to the same value b [12]. For the sake of pedagogy, we give here the expression of ϕ at leading order in the weak-coupling regime [14] when $x>b$ and $x'>b$,

$$\begin{aligned}\phi^{(0)}_{IV}(x,x',\mathbf{k})=&\frac{2\pi}{\sqrt{\kappa_D^2+\mathbf{k}^2}}e^{-|x-x'|\sqrt{\kappa_D^2+\mathbf{k}^2}}\\&+Z^{(0)}_{IV}(|\mathbf{k}|)e^{-(x+x')\sqrt{\kappa_D^2+\mathbf{k}^2}}\end{aligned} \tag{44}$$

with

$$\begin{aligned}Z^{(0)}_{IV}(|\mathbf{k}|)=&\frac{2\pi}{\sqrt{\kappa_D^2+\mathbf{k}^2}}e^{2b\sqrt{\kappa_D^2+\mathbf{k}^2}}\\&\times\frac{\kappa_D^2-\Delta_{\mathrm{el}}e^{-2b|\mathbf{k}|}(\sqrt{\kappa_D^2+\mathbf{k}^2}+|\mathbf{k}|)^2}{(\sqrt{\kappa_D^2+\mathbf{k}^2}+|\mathbf{k}|)^2-\Delta_{\mathrm{el}}e^{-2b|\mathbf{k}|}\kappa_D^2}.\end{aligned} \tag{45}$$

These expressions have been derived in the case $\Delta_{\mathrm{el}}=0$ and $b=0$ in Ref. [6] and in the case $\Delta_{\mathrm{el}}\neq0$ and $b=0$ in Ref. [7]. [We notice that b can be set to 0 only when the electrostatic response of the wall is repulsive [11], namely, when $\epsilon_{\mathrm{W}}<\epsilon_{\mathrm{solv}}$ ($\Delta_{\mathrm{el}}<0$).] Explicit calculations in confined geometries are done in Ref. [8]. All these leading-order results correspond to uniform density profiles in the region $x>b$.

As a consequence of Eqs. (37), (38), (40), and (43), the small-$\mathbf{k}$ expansion of ϕ also contains a $|\mathbf{k}|$-term,

$$\phi(x,x',\mathbf{k})=\phi(x,x',\mathbf{k}=\mathbf{0})+|\mathbf{k}|B^{[1]}_{\phi}(x,x')+O(\mathbf{k}^2), \tag{46}$$

where $B^{[1]}_{\phi}(x,x')$ takes different forms when x and x' are in regions I,II,III,IV, respectively. $B^{[1]}_{\phi}(x,x')$ is continuous everywhere as $\phi(x,x',\mathbf{k})$ is. The discontinuity of $\partial\phi(x,x',\mathbf{k})/\partial x$ at $x=x'$ is given by the part $\phi_{\mathrm{sing}}(x,x',\mathbf{k}^2)$ in $\phi(x,x',\mathbf{k})$. Henceforth $\partial B^{[1]}_{\phi}(x,x')/\partial x$ is continuous at

$x=x'$, and the continuity of $\partial\phi(x,x',\mathbf{k})/\partial x$ at the various planes $x=b_i$ when $x\neq x'$ implies the continuity of $\partial B_\phi^{[1]}(x,x')/\partial x$ at every $x=b_i$. Moreover, $B_\phi^{[1]}(x,x')$ vanishes when x or x' goes to $+\infty$, as $\phi(x,x',\mathbf{k})$ does.

The fact that the small-$\mathbf{k}$ expansion of the Fourier transform of $\phi(x,x',\mathbf{y})$ contains some terms that are not analytic in the Cartesian components of $\mathbf{k}$ signals the existence of algebraic tails in the large-$\mathbf{y}$ behavior of $\phi(x,x',\mathbf{y})$. Since the nonanalytic term with the lowest order in powers of $|\mathbf{k}|$ is proportional to $|\mathbf{k}|=\sqrt{k_1^2+k_2^2}$ (where k_1 and k_2 are the Cartesian components of $\mathbf{k}$), the slowest algebraic tail decays as $1/y^3$. Its coefficient reads (see p. 363 of Ref. [22])

$$\phi(x,x',\mathbf{y}) \underset{|\mathbf{y}|\to+\infty}{\sim} \frac{f_\phi(x,x')}{|\mathbf{y}|^3} \tag{47}$$

for $x>b_{\min}$ and $x'>b_{\min}$ with

$$f_\phi(x,x')=-\frac{1}{2\pi}B_\phi^{[1]}(x,x'), \tag{48}$$

$1/y^3$ tails have also been exhibited in expressions for $\phi^{(0)}$ in various confined geometries [8].

According to Eq. (41), $B_{\phi_{IV}}^{[1]}(x,x')$ has the factorized structure

$$B_{\phi_{IV}}^{[1]}(x,x')=B_{Z_{IV}}^{[1]}h_{IV}^{+}(x,\mathbf{k}^2=0)h_{IV}^{+}(x',\mathbf{k}^2=0) \quad \text{if } x>b_{\max} \text{ and } x'>b_{\max}. \tag{49}$$

[We notice that, since $h^+(x,\mathbf{k}^2=0)$ is a solution of Eq. (39), which tends to zero when x goes to infinity, $h^+(x,\mathbf{k}^2=0)$ has the same sign for any x.]

More generally, when x and x' are in regions III or IV $B_\phi^{[1]}(x,x')$ has an expression given by Eq. (40) where $Z_{(ii')}^{\pm\pm}$ is replaced by $B_{Z_{(ii')}^{\pm\pm}}^{[1]}$ and $\mathbf{k}^2$ is set equal to 0. Since $h^+(x,\mathbf{k}^2=0)$ and $h^-(x,\mathbf{k}^2=0)$ are solutions of Eq. (39), $f_\phi(x,x')$, defined for $x>b_{\min}$ and $x'>b_{\min}$ and proportional to $B_\phi^{[1]}(x,x')$ [see Eq. (48)], obeys the following equation:

$$\frac{\partial^2 f_\phi(x,x')}{\partial x^2}=\bar{\kappa}^2(x)f_\phi(x,x'). \tag{50}$$

Moreover, for any given $x'>b_{\min}$, $f_\phi(x,x')$ vanishes at large positive x, as it is the case for $B_\phi^{[1]}(x,x')$. As a consequence, for any given x', $f_\phi(x,x')$ has the same sign for every $x>b_{\min}$. The result also holds when the roles of x and x' are exchanged. Therefore, $f_\phi(x,x')$ has the same sign for any x or x' larger than $b_{\min}$, as written in Eq. (6).

C. Repulsive nature of the $1/y^3$ tail of ϕ

Now, in order to determine the sign of $f_\phi(x,x')$, we show that $\phi(x,x',\mathbf{k}=\mathbf{0})$ obeys a sum rule, as well as $f_\phi(x,x')$. These sum rules hold for any solution of Eq. (35) with boundary conditions recalled after Eq. (26), whatever the function $\bar{\kappa}^2(x)$ with finite steps may be.

First, the sum rule for $\phi(x,x',\mathbf{k}=\mathbf{0})$ reads

$$\int_0^\infty dx\,\bar{\kappa}^2(x)\,\phi(x,x',\mathbf{k}=\mathbf{0})=4\pi \quad \text{if } x'>b_{\min}. \tag{51}$$

(We notice that the lower bound 0 of the integral in Eq. (51) can be replaced by $b_{\min}$, because $\bar{\kappa}^2(x)$ vanishes in the range $0<x<b_{\min}$.) The derivation of Eq. (51) is the following. $\phi(x,x',\mathbf{k}=\mathbf{0})$ obeys Eq. (35) with $\mathbf{k}^2=\mathbf{0}$, and $\partial\phi(x,x',\mathbf{k})/\partial x$ vanishes when x goes to infinity for any $\mathbf{k}$. Moreover, for $x'>b_{\min}$ $\partial\phi(x,x',\mathbf{k}=\mathbf{0})/\partial x$ at $x=0^+$ is given in terms of the same derivative at $x=0^-$ by boundary condition (29). $\partial\phi(x,x',\mathbf{k}=\mathbf{0})/\partial x$ vanishes for $x<0$, by virtue of the explicit expression (37), which is valid for any $\bar{\kappa}^2(x)$, and so does $\partial\phi(x,x',\mathbf{k}=\mathbf{0})/\partial x$ at $x=0^+$.

We notice that in a linearized mean-field approximation $h_{\alpha\alpha'}(x,x',\mathbf{y})$ can be replaced by $F^{\mathrm{cc}}=-\beta e_\alpha e_{\alpha'}\phi(x,x',\mathbf{y})$. Sum rule (51) implies that this approximated expression for $h_{\alpha\alpha'}(x,x',\mathbf{y})$ does obey the local-electroneutrality sum rule satisfied by the exact $h_{\alpha\alpha'}(x,x',\mathbf{y})$,

$$e_\alpha=-\int d\mathbf{r}'\sum_{\alpha'} e_{\alpha'}\rho_{\alpha'}(\mathbf{r}')h_{\alpha\alpha'}(\mathbf{r},\mathbf{r}'). \tag{52}$$

(See Ref. [5] for a review of the sum rules.)

The sum rule for $f_\phi(x,x')$ arises from similar arguments. By virtue of Eq. (50) and since $\partial f_\phi(x,x')/\partial x$ vanishes when x goes to infinity [since $B_\phi^{[1]}(x,x')$ vanishes as well as ϕ at large x],

$$\int_{b_{\min}}^\infty dx\,\bar{\kappa}^2(x)f_\phi(x,x')=-\left.\frac{\partial f_\phi(x,x')}{\partial x}\right|_{x=b_{\min}^+}. \tag{53}$$

The rhs of Eq. (53) is determined by the fact that $f_\phi(x,x')$ is proportional to $B_\phi^{[1]}(x,x')$ in regions III and IV by virtue of Eq. (48). $B_\phi^{[1]}(x,x')$ is defined everywhere through Eq. (46) and its partial derivative with respect to x is continuous at $x=b_{\min}$. The explicit solution (38) for $\phi(x,x',\mathbf{k})$ when x is in region II and $x'>b_{\min}$ exhibits the following property,

$$\frac{\partial B_\phi^{[1]}(x,x')}{\partial x}=\frac{\epsilon_W}{\epsilon_{\mathrm{solv}}}\phi(x,x',\mathbf{k}=\mathbf{0}) \quad \text{if } 0<x<b_{\min}(x'>b_{\min}). \tag{54}$$

[When x and x' are in the range specified in Eq. (54), $\phi(x,x',\mathbf{k}=\mathbf{0})$ is independent of x and relation (54) has its root in the boundary conditions for ϕ at $x=0$.] Since $\phi(x,x',\mathbf{k})$ is continuous at $x=b_{\min}$ for any value of $\mathbf{k}$, the rhs of Eq. (53) is equal to $1/(2\pi)$ times $(\epsilon_W/\epsilon_{\mathrm{solv}})\phi(x,x',\mathbf{k}=\mathbf{0})|_{x=b_{\min}^+}$. According to first sum rule (51), the integration of $\bar{\kappa}^2(x')$ times Eq. (53) leads to the second sum rule

$$\int_{b_{\min}}^\infty dx\int_{b_{\min}}^\infty dx'\,\bar{\kappa}^2(x)\bar{\kappa}^2(x')f_\phi(x,x')=2\frac{\epsilon_W}{\epsilon_{\mathrm{solv}}}. \tag{55}$$

We notice that, if $h_{\alpha\alpha'}(x,x',y)$ is again approximated by the bond $F^{\mathrm{cc}}=-\beta e_\alpha e_{\alpha'}\phi(x,x',y)$, then Eq. (55) implies

that the corresponding approximation $-\beta e_\alpha e_{\alpha'} f_\phi(x,x')$ for the coefficient $-\beta f_{\alpha\alpha'}(x,x')$ of the $1/y^3$ tail of $h_{\alpha\alpha'}(x,x',y)$ does obey sum rule (4).

Since $f_\phi(x,x')$ has the same sign for any x or x' larger than $b_{\min}$ and obeys sum rule (55) where $\bar{\kappa}^2(x)$ and $\bar{\kappa}^2(x')$ are positive, we conclude that

$$f_\phi(x,x')>0. \tag{56}$$

In other words, for any function $\bar{\kappa}^2(x)$, the $1/y^3$ tail of the screened potential $\phi(x,x',\mathbf{y})$ is repulsive at all distances x and x' (larger than $b_{\min}$).

D. Factorization of the $1/y^3$ tail of ϕ

When x and x' are larger than $b_{\max}$, $f_\phi(x,x')$ has the factorized structure given by Eqs. (48) and (49). $B^{[1]}_{Z_{IV}}$ has the same sign as $B^{[1]}_{\phi_{IV}}(b_{\max},b_{\max})$. $B^{[1]}_{\phi_{IV}}(b_{\max},b_{\max})<0$ by virtue of Eq. (48) and of the positive sign of $f_\phi(x,x')$ for any x and x' [see Eq. (56)]. As a consequence, for x and x' larger than $b_{\max}$, the $1/y^3$ tail of $\phi(x,x',\mathbf{y})$ has the dipolar structure written in Eq. (7), where $\bar{D}_\phi(x)$ is defined up to an arbitrary sign ε,

$$\bar{D}_\phi(x)=\varepsilon\sqrt{\frac{(-B^{[1]}_{Z_{IV}})}{2\pi}}h^+_{IV}(x,\mathbf{k}^2=\mathbf{0}), \tag{57}$$

$\bar{D}_\phi(x)$ has the same sign for any x, as well as $h^+_{IV}(x,\mathbf{k}^2=\mathbf{0})$.

IV. CORRELATIONS AT LARGE DISTANCES ALONG THE WALL

A. $1/y^3$ decay of correlations

The leading $f_\phi(x,x')/y^3$ tail of the screened potential ϕ, where $f_\phi(x,x')$ is integrable, induces the same power-law decay for the Ursell function $h_{\alpha\alpha'}$. The argument is the following. Since ϕ falls off as $1/y^3$ at large distances $|\mathbf{y}|$, bonds F^{cc} and F_R in resummed Mayer diagrams decay as $1/y^3$ and $1/y^6$, respectively, according to Eqs. (23) and (24). In graph decomposition (30) of $h_{\alpha\alpha'}$ where bonds are F^{cc} and I, the topology of diagrams involved in I implies that I decays at large distances y at least as $1/y^6$ (see Sec. II E). Then, in the series representations of $h^{cc}_{\alpha\alpha'}$, $h^{-c}_{\alpha\alpha'}$, $h^{c-}_{\alpha\alpha'}$ and $h^{--}_{\alpha\alpha'}$ shown in Figs. 1–3, every term, except I, has $1/y^3$ tails arising from all F^{cc} bonds in the series.

Indeed, all graphs in Figs. 1–3 are chain graphs, so that their leading algebraic tail must be determined as follows. Because of the translational invariance in the direction parallel to the wall, graphs in Figs. 1–3 can be seen as multiple convolutions with respect to the variable $\mathbf{y}$, which are integrated over every x variable with a weight $w(x)$. The Fourier transform in direction $\mathbf{y}$ of a single convolution takes the form

$$C(x,x',\mathbf{k})\equiv\int dx''f(x,x'',\mathbf{k})w(x'')g(x'',x',\mathbf{k}). \tag{58}$$

If $f(x,x'',\mathbf{y})$ decays as $1/y^3$, whereas $g(x'',x',\mathbf{y})$ falls off faster than $1/y^3$, then the term in the $\mathbf{k}$ expansion of $C(x,x',\mathbf{k})$ that is nonanalytic in the components of $\mathbf{k}$ at the lowest order in powers of $|\mathbf{k}|$ comes from the corresponding term $|\mathbf{k}|B^{[1]}_f(x,x'')$ in the $\mathbf{k}$ expansion of $f(x,x'',\mathbf{k})$ and is equal to

$$|\mathbf{k}|\int dx''B^{[1]}_f(x,x'')w(x'')g(x'',x',\mathbf{k}=\mathbf{0}). \tag{59}$$

Then, the formula already used to get Eqs. (47) and (48) from Eq. (46) leads to

$$C(x,x',\mathbf{y})\underset{|\mathbf{y}|\to+\infty}{\sim}-\frac{1}{2\pi}\frac{1}{|\mathbf{y}|^3}\int dx''B^{[1]}_f(x,x'')w(x'')\times g(x'',x',\mathbf{k}=\mathbf{0}). \tag{60}$$

When both f and g behave as $1/y^3$, the $\mathbf{k}$ expansion of $C(x,x',\mathbf{k})$ involves two nonanalytic terms at order $|\mathbf{k}|$ and the integral in Eq. (60) is replaced by

$$\int dx''B^{[1]}_f(x,x'')w(x'')g(x'',x',\mathbf{k}=\mathbf{0})+\int dx''f(x,x'',\mathbf{k}=\mathbf{0})w(x'')B^{[1]}_g(x'',x'). \tag{61}$$

The argument can be generalized to a convolution involving several functions that all decay as $1/y^3$. (Similar considerations for convolutions of algebraically decaying functions have already been displayed in Ref. [19].)

B. Dipolar structure of the $1/y^3$ tail

The formal structure of the $1/y^3$ tail of the Ursell function $h_{\alpha\alpha'}(x,x',\mathbf{y})$ can be derived by using decomposition (30) together with the fundamental properties (60) and (61). Let us call $h^{\cdot\cdot}_m(x,x',\mathbf{y},\alpha,\alpha')$ the graph with m bonds F^{cc} in the representations of either h^{cc}, h^{c-}, h^{-c} or h^{--} exhibited in Figs. 1–3. According to Eq. (61), the various $1/y^3$ tails of every graph $h^{\cdot\cdot}_m$ are determined by replacing one of the bonds F^{cc} by its $1/y^3$ behavior at large y, whereas the other part of the graph is replaced by its Fourier transform at the value $\mathbf{k}=\mathbf{0}$ (while integrations over variables x's are left unchanged).

As a consequence, as shown in Appendix, when all species have the same closest approach distance to the wall, the dipolar structure (7) of the $1/y^3$ tail of the screened potential $\phi(x,x',\mathbf{y})$ induces that $h_{\alpha\alpha'}(x,x',\mathbf{y})$ also has a dipolar structure (8) with

$$D_\alpha(x)=\frac{e}{\sqrt{\epsilon_{solv}}}\{Z_\alpha[\bar{D}_\phi(x)+\bar{C}^{c-}(x)]+C^{--}_\alpha(x)\}, \tag{62}$$

where $\bar{C}^{c-}(x)$ and $C^{--}_\alpha(x)$ are defined in Eqs. (A10) and (A6), respectively. The term in braces in Eq. (62) can be rewritten as

$$Z_\alpha \bar{D}_\phi(x) + \int d\mathbf{r}'' \sum_{\gamma''} \rho_{\gamma''}(x'') Z_{\gamma''} \bar{D}_\phi(x'') [h^{c-}_{\alpha\gamma''}(\mathbf{r},\mathbf{r}'') + h^{--}_{\alpha\gamma''}(\mathbf{r},\mathbf{r}'')]. \quad (63)$$

In the weak-coupling limit, only a finite number of resummed Mayer diagrams contribute to the coefficient D_α. The calculation performed up to the first-order correction in the forthcoming paper [12] shows that the latter coefficient does not vanish.

We stress that results (6)–(8) are valid for species with various excluded-volume sizes. Indeed, if all species have not the same hard-core size, the difference appears in the short-ranged potentials $v_{SR}(|\mathbf{r}-\mathbf{r}'|;\alpha,\alpha')$ and $V_{SR}(x;\alpha)$, which describe repulsive pairwise interactions and the impenetrability of the wall, respectively. According to its definition (21), the potential $\phi(\mathbf{r},\mathbf{r}')$ may depend on $v_{SR}(|\mathbf{r}-\mathbf{r}'|;\alpha,\alpha')$ and $V_{SR}(x;\alpha)$ only through the explicit expression of $\bar{\kappa}^2(x)$. The generic properties of the coefficient $f_\phi(x,x')$ derived in Sec. III rely only on the positive sign of $\bar{\kappa}^2(x)$ and on the boundary conditions obeyed by ϕ. Besides, the detailed form of $v_{SR}(|\mathbf{r}-\mathbf{r}'|;\alpha,\alpha')$ involved in bond F_R never comes up in the discussion of the structure of correlations at large distances y.

We recall that, as stressed in Sec. III B, the existence of a $f_\phi(x,x')/y^3$ tail for $\phi(x,x',y)$ does not depend on the specific form of $V_{SR}(x;\alpha)$ as long as $\bar{\kappa}^2(x)$ vanishes when $x<0$. By virtue of the same argument as that used in previous paragraph, the generic properties of the latter tail, as well as the subsequent property (8) for the $1/y^3$ tail of $h_{\alpha\alpha'}(x,x',y)$, are valid even if $V_{SR}(x;\alpha)$ is a soft repulsive potential instead of hard-core repulsion (14).

V. GENERALIZATION OF PREVIOUS RESULTS

The main results (6)–(8) namely, the repulsive nature of the $1/y^3$ tail of ϕ, which is always true, and the dipolar structures of the $1/y^3$ tails of ϕ and $h_{\alpha\alpha'}$, which arise only in some cases, also hold in the following different situations.

A. Wall with surface charge

If the wall carries an external surface charge, by virtue of the superposition principle for solutions of the Poisson equation, one can choose to write the total electrostatic energy as the sum of two contributions: on one hand the one-body interactions of all fluid charges with the electrostatic potential created by the external charge on the wall and by the electrostatic response of the wall, and on the other hand Coulomb pair interactions (9), which take into account the electrostatic response of the wall, but which are independent of the external charge. It can be shown, as detailed in a forthcoming paper, that some generalized Mayer diagrams can be introduced as in Sec. II. (The effect of the surface charge is dealt with thanks to a generalized fugacity in a way similar to what is done for the electrostatic response of the glass wall in Ref. [14].) Then the density profiles can be studied. In the Mayer representation of the Ursell function, an auxiliary potential ϕ, which obeys the inhomogeneous Debye equation (25), appears after systematic resummations of the Coulomb divergences.

The resummed electrostatic potential ϕ obeys the same boundary conditions as the Coulomb pair interaction [see Eq. (21)], and these conditions are independent of the external charge. Henceforth, in the determination of ϕ the existence of the wall surface charge comes up only in the equation obeyed by ϕ, where it arises in the function $\bar{\kappa}^2(x)$ through density profiles [see Eq. (26)]. The whole argument developed through Secs. III and IV is valid. Indeed, only the positive sign of $\bar{\kappa}^2(x)$ and the boundary conditions obeyed by ϕ do matter in the proof of the repulsive nature (6) of the $1/y^3$ tail of the screened potential ϕ, while dipolar structures (7) and (8) are not altered by the precise form of $\bar{\kappa}^2(x)$. Therefore, these results hold in the presence of an external surface charge on the wall.

B. Beyond point charges

If some species, for instance, $\alpha=n_s$, are made of colloidal spherical particles, one has to take into account not only its mesoscopic excluded-volume size (already incorporated in the primitive model) but also the fact that its charge is not concentrated at the center of the particle but spread on its surface. The microscopic Coulomb potential between two species coincides with expression (9) only for relative distances $|\mathbf{r}-\mathbf{r}'|$ larger than the sum of their radii. Since the integral equation (21) obeyed by $\phi(\mathbf{r},\mathbf{r}')$ does not involve the short-ranged pairwise potential $v_{SR}(|\mathbf{r}-\mathbf{r}'|;\alpha,\alpha')$ but only the electrostatic interaction $v(\mathbf{r},\mathbf{r}')$, it describes resummed interactions between *penetrable* spheres with uniform surface charges spread on them for $\alpha=n_s$ and point charges for other species.

Then the solution for ϕ in the bulk is no longer Eq. (28). However, its large $|\mathbf{r}-\mathbf{r}'|$ behavior is expected to take the Debye form (28) with a "geometric" corrective factor, as it is the case for the large $|\mathbf{r}-\mathbf{r}'|$ decay of the bulk effective interaction between two *impenetrable* spheres with uniform surface charges [see, e.g., Ref. [24] for a detailed calculation of the expression recalled in Eq. (65)]. Similarly, the solution in the vicinity of the wall is also altered by the fact that some charges are distributed uniformly over spheres.

The resolution of the corresponding problems for penetrable spheres (in the bulk or near the wall) is far beyond the scope of the present paper. However, when y is large with respect of the size of spherical charges, the monopole-monopole part of $v(\mathbf{r},\mathbf{r}')$ yields the leading tail in their effective screened interactions, and functional forms (6) and (7) of the large-y behavior of $\phi(x,x',y)$ should not be changed.

VI. EXPERIMENTS WITH COLLOIDS

Most colloidal particles acquire a charge either from surface charge groups or by specific adsorption from an electrolytic solution. We call $Z_{col}e$ the bare solvated (or "structural") charge, which arises from the intricate mechanism of solvatation. In the past decade colloidal suspensions have

been widely studied experimentally, in particular, because, apart from their numerous industrial applications, they can be seen as model systems for structural phase transitions.

It is well known that the effective interaction $u^{B}_{col\ col}$ between two isolated colloidal particles in the bulk is well mimicked by the DLVO (Derjaguin-Landau-Verwey-Overbeek) potential [23]. (In the following, the superscript B will denote bulk quantities.) When colloids are separated by more than a few screening lengths, the screened Coulomb interaction between the two uniformly charged spheres dominates the other contribution in the DLVO interaction. The latter Coulomb interaction is calculated in a linearized mean-field approximation [24] (namely, linearized Poisson-Boltzmann theory) and the result at relative distances y large with respect to the screening length and the charge sizes yields the formula recalled in Eq. (65).

A. Sketch of the debate

From the experimental point of view, the main advantage of colloids is that their mesoscopic size allows one to track the motion of *every* colloidal sphere with a conventional optical microscope and a video camera. Thus, the correlation $h_{col\ col}$ can be experimentally assessed for colloids when they are far away from the vessel walls or when they are confined between two glass plates or in the vicinity of a single plane surface. (See references quoted in Ref. [4].)

In particular, in 1997 Larsen and Grier experimentally determined the correlation $h_{col\ col}$ between dilute negatively charged polystyrene sulphate spheres optically trapped at the same distance x from a glass wall with some negative charge on its surface [2]. Since colloids are dilute in the experiment, $w_{col\ col}$ defined in Eq. (1) is expected to coincide, in fact, with the effective interaction for an isolated pair, namely, with the immersion free energy of two isolated colloidal particles in a bath made of ions. (We recall that $w_{col\ col}$ is a statistical average performed over microscopic configurations of both microscopic ions and many colloidal particles, whereas the immersion free energy $u_{col\ col}$ of two colloidal spheres arises from averaging only over counterion configurations.) The authors claimed that the corresponding effective pairwise interaction $u_{col\ col}(x,x',y)$ between mesoscopic like charges at the same distance $x=x'$ from the wall was attractive at large relative distances y.

However, theoretical works devoted to the effective interaction $u_{col\ col}$ between two isolated colloids predicted that $u_{col\ col}$ is repulsive not only in the bulk but even in a confined geometry. [These works involve mean-field (Poisson-Boltzmann) theories [25] or local density functional approximations where correlations are included in a local free-energy term [26].] Theoretical results about the repulsive nature of $u_{col\ col}$ were supported by a second experiment in the vicinity of a single charged glass wall published in 2001 by Behrens and Grier [27]. In the experiment, denser silica spheres are confined at a fixed distance from the wall by the balance between gravity and the electrostatic repulsion exerted by the surface charge on the wall. Colloidal particles are not dilute, and oscillations in $w_{col\ col}$, the depth of which depends on the colloid density, appear over a length scale equal to a few nearest-neighbor distances. Behrens and Grier argued that the observed oscillations should be ascribed to a mere crowding effect commonly seen in liquids even when the electrostatic part of the immersion free energy of an isolated pair $u_{col\ col}$ is repulsive.

Eventually, Squires and Brenner [3] argued that the attraction determined in the first experiment [2] could be accounted for by a nonequilibrium effect: the measured quantity was, in fact, the sum of the repulsive equilibrium free energy $u_{col\,col}$ and an attractive phenomenological attraction $u^{hyd}_{col\ col}$, which results from hydrodynamic flows excited by the spheres retreat from the charged wall, whose charge has the same sign as that of colloids.

However, attraction between like charges has also been observed in experiments with colloidal suspensions confined between two charged walls, and in the latest ones [4], which involve experimental methods similar to those used in Refs. [2] and [27], Han and Grier have checked the absence of any hydrodynamical effect. Therefore, an open question is: in the absence of any hydrodynamical effect, might confinement combined with many-body effects mediated by colloids or ions result into an attractive effective pairwise interaction $w_{col\ col}$ or $u_{col\ col}$ in some range of distances?

B. Experiment about dilute colloids in the vicinity of a single wall

In the present section we revisit the case of the vicinity of a single wall studied in Ref. [2] in the light of our results about statistical mechanics of charge fluids. In the experiment of Ref. [2], the diameter of polystyrene sulphate spheres is $\sigma_{col}=0.652\ \mu$m, and the mean intercolloid distance a_{col} is greater than 25 μm. At room temperature T, the Bjerrum length $\lambda\equiv\beta e^2/\epsilon_{solv}$ (closest approach distance between like-charge ions with mean kinetic energy $1/\beta$) is $\lambda=7\ 10^{-4}\ \mu$m. The absolute value $|Z_{col}|$ of the bare solvated charge in electron-charge units is estimated to be much smaller than 10^5, which is the number of ionizable sulphate groups chemically bound to its surface before solvatation, because not all sulphate groups dissociate.

The correlation $h_{col\ col}$ between colloidal particles is measured at distances $x_1=9.5\pm1.0\ \mu$m and $x_2=2.5\pm0.5\ \mu$m for relative distances y, which vary from 2.3 μm to 7 μ m. $w_{col\ col}$ at x_1 is always repulsive, whereas at x_2 it becomes attractive for distances $y\geqslant y_{inv}=2.5\ \mu$m.

Colloids are dilute enough for the parameter σ_{col}/a_{col} to be small ($\sigma_{col}/a_{col}<0.03$). Thus we expect that, in the range of investigated y's, which are indeed larger than the colloid diameter σ_{col}, the functional form of $w_{col\,col}(x,x',y)$ is determined only by interactions different from the hard-core repulsion. We recall that this is not true in the experiment of Ref. [27] where the ratio σ_{col}/a_{col} takes the high value 0.5. Then, because of crowding effects, the dependance of $w_{col\,col}(x=x',y)$ upon the relative distance y has oscillations with a period equal to the nearest-neighbor distance $2\sigma_{col}$ up to y of order $8\sigma_{col}$ [see the comment after Eq. (1)].

1. Effective electrostatic interaction in the bulk

In the bulk, when the relative distance y between colloids is larger than the screening length κ_B^{-1}, we expect that the

effective pairwise interaction is dominated by the Coulomb forces and, when y is also large with respect to the colloid radius, it takes the Debye form

$$w^{\mathrm{B}}_{\mathrm{col\,col}}(y) \underset{(\kappa_{\mathrm{B}}^{-1},\sigma_{\mathrm{col}})<y}{\sim} \frac{[Z^{\mathrm{eff\,B}}_{\mathrm{col}}e]^2}{\epsilon_{\mathrm{solv}}}\frac{e^{-\kappa_{\mathrm{B}}y}}{y}. \tag{64}$$

The difference between $Z^{\mathrm{eff\,B}}_{\mathrm{col}}$ and the ''bare'' solvated charge Z_{col} defined at the beginning of Sec. VI arises from the combination of many-body effects (linked to the Coulomb coupling and short-ranged repulsions) with the steric effect due to the fact that the charge is not concentrated at a point but is spread over a sphere.

When colloids are *very dilute*, many-body interactions between colloids become negligible and $w_{\mathrm{col\ col}}$ tends to the immersion free energy $u_{\mathrm{col\ col}}$ of an isolated pair of colloids, where many-body effects are only due to interactions mediated by ions. Since functional form (64) of $w^{\mathrm{B}}_{\mathrm{col\ col}}(y)$ involves size effects only in the parameters $Z^{\mathrm{eff\,B}}_{\mathrm{col}}$ and κ_{B}, $u^{\mathrm{B}}_{\mathrm{col\ col}}(y)$ has the same functional form as $w^{\mathrm{B}}_{\mathrm{col\ col}}(y)$, where κ_{B} is replaced by $\kappa^{\mathrm{ion}}_{\mathrm{B}}$, the inverse screening length created by ions, and $Z^{\mathrm{eff\,B}}_{\mathrm{col}}$ is replaced by $Z^{\mathrm{eff\ B\ ion}}_{\mathrm{col}}$.

In the DLVO approximation, which is usually used for $u^{\mathrm{B}}_{\mathrm{col\ col}}$ in order to interpret experiments with colloids, $\kappa^{\mathrm{ion}}_{\mathrm{B}}$ is approximated by the inverse ionic Debye length $\kappa^{\mathrm{ion}}_{D}$, while the effective charge $Z^{\mathrm{eff\ B\ ion}}_{\mathrm{col}}$ is approximated by $Z^{\mathrm{DLVO}}_{\mathrm{col}}$,

$$u^{\mathrm{B\ DLVO}}_{\mathrm{col\ col}}(y) \underset{(1/\kappa_D^{\mathrm{ion}},\sigma_{\mathrm{col}})<y}{\sim} \frac{[Z^{\mathrm{DLVO}}_{\mathrm{col}}e]^2}{\epsilon_{\mathrm{solv}}}\frac{e^{-\kappa_D^{\mathrm{ion}}y}}{y}. \tag{65}$$

In Eq. (65) $\kappa^{\mathrm{ion}}_{D}$ is defined as in Eq. (27) with the summation restricted to ionic species, and $Z^{\mathrm{DLVO}}_{\mathrm{col}}$ is equal to Z_{col} times a ''geometric'' factor [24]:

$$Z^{\mathrm{DLVO}}_{\mathrm{col}} = Z_{\mathrm{col}}\frac{e^{\kappa_D^{\mathrm{ion}}\sigma_{\mathrm{col}}/2}}{1+(\kappa_D^{\mathrm{ion}}\sigma_{\mathrm{col}}/2)}. \tag{66}$$

We notice that, as a result of the strong electrostatic coupling between microions and the macroscopic charge of a colloid in the vicinity of the colloid surface, nonlinearities and microion correlations can dramatically reduce $Z^{\mathrm{eff\ B\ ion}}_{\mathrm{col}}$ with respect to the bare solvated value Z_{col} (see, e.g., Ref. [28]). When the structural charge Z_{col} increases, $Z^{\mathrm{eff\ B\ ion}}_{\mathrm{col}}$ may even tend to a saturation value independent of Z_{col} and proportional to the diameter σ_{col} [29].

2. Experimental results in the bulk

At distance $x_1 = 9.5\ \mu$m the experimental curve is properly fitted by Eq. (64). The latter fit determines the values of the inverse screening length κ_{B} and of the effective charge $Z^{\mathrm{eff\,B}}_{\mathrm{col}}$ in the bulk. Their respective values are $\kappa_{\mathrm{B}}^{-1} = 0.275\ \mu$m and $Z^{\mathrm{eff\,B}}_{\mathrm{col}} = 11\,000$. Henceforth

$$\sigma_{\mathrm{col}} = 2.4\,\kappa_{\mathrm{B}}^{-1}. \tag{67}$$

If expression (64) with measured parameters is identified with its approximate DLVO value (65), then $\kappa^{\mathrm{ion}}_{D} \sim \kappa_{\mathrm{B}}$ and Z_{col} is of the same order as $Z^{\mathrm{eff\,B}}_{\mathrm{col}}$: $|Z_{\mathrm{col}}| = 7300$. The latter value is indeed lower than the number 10^5 of ionizable groups on the colloid surface before solvatation.

The values derived from the fit give various pieces of information. First, experiments are carried at distances from the wall equal to $x_1 \sim 35\kappa_{\mathrm{B}}^{-1}$, which is indeed far away in the bulk, and $x_2 \sim 9\kappa_{\mathrm{B}}^{-1}$, while the relative distance y ranges from about $8\kappa_{\mathrm{B}}^{-1}$ to $25\kappa_{\mathrm{B}}^{-1}$.

Henceforth distances y are large compared with the screening length κ_{B}^{-1} and the colloid diameter $\sigma_{\mathrm{col}} \sim 2.4\kappa_{\mathrm{B}}^{-1}$: they are indeed in the range where electrostatic forces are expected to dominate other short-ranged interactions between colloidal particles, and where the monopole-monopole part of electrostatic interactions is indeed the leading term.

Another information can be checked from the fit: the Coulomb coupling between colloidal particles is strong. The ''bare'' Coulomb coupling parameter $\Gamma_{\mathrm{col\ col}} \equiv \beta[Z_{\mathrm{col}}e]^2/(\epsilon_{\mathrm{solv}}a_{\mathrm{col}}) = Z^2_{\mathrm{col}}(\lambda/a_{\mathrm{col}})$ ranges from 370 to 1500 when the mean intercolloid distance a_{col} varies from 100 μm to 25 μm. Meanwhile the effective Coulomb parameter $[Z^{\mathrm{eff\,B}}_{\mathrm{col}}]^2\kappa_{\mathrm{B}}\lambda$, which we define from $\Gamma_{\mathrm{col\ col}}$ by replacing Z_{col} by $Z^{\mathrm{eff\,B}}_{\mathrm{col}}$ and a_{col} by κ_{B}^{-1}, is of order 10^5, since the effective Coulomb parameter $\kappa_{\mathrm{B}}\lambda$ between ions is of order 10^{-3}. This effective parameter arises in

$$\frac{w^{\mathrm{B}}_{\mathrm{col\ col}}(y)}{k_{\mathrm{B}}T} \underset{(\kappa_{\mathrm{B}}^{-1},\sigma_{\mathrm{col}})<y}{\sim} [Z^{\mathrm{eff\,B}}_{\mathrm{col}}]^2\tilde{\lambda}\frac{e^{-\tilde{y}}}{\tilde{y}}, \tag{68}$$

where $\tilde{y} = \kappa_{\mathrm{B}}y$ and $\tilde{\lambda} = \kappa_{\mathrm{B}}\lambda$. (Weak-coupling expansions are series in powers of $\tilde{\lambda}$ times possible logarithms. $\tilde{\lambda}$ is sometimes called the plasma parameter.)

However, we notice that, since the distances y investigated in the experiment are larger than $8\kappa_{\mathrm{B}}^{-1}$, the large intensity of the Coulomb interaction given by $[Z^{\mathrm{eff\,B}}_{\mathrm{col}}]^2\tilde{\lambda}$ is exponentially reduced by the screening effect contained in $\exp[-\tilde{y}]$: $w^{\mathrm{B}}_{\mathrm{col\ col}}(y)$ is of order $k_{\mathrm{B}}T$ at $y \sim 10\,\kappa_{\mathrm{B}}^{-1}$.

3. Dilute colloids in the vicinity of the wall: modelization from statistical mechanics of charge fluids

We stress that our model is relevant for the experimental system of Ref. [2]. First, at the investigated distances y the electrostatic force dominates other interactions, as previously checked in the bulk. Second, our model takes into account the characteristic steric and electrostatic features of the experiment. On one hand, all species do not have the same closest approach distance to the wall, and they have different sizes (see Sec. II A). (The closest approach distance b_{col} of colloids to the wall is at least of order $\sigma_{\mathrm{col}}/2$: it is very different from the corresponding distance b_{ion} for microscopic ions.) On the other hand, the existence of a negative surface charge on the glass wall, and the fact that the charge of one species is not concentrated at a point but spread on a sphere have been discussed in the generalizations of Sec. V.

If $b_{\mathrm{col}} \sim \sigma_{\mathrm{col}}/2$, the leading term in the effective electrostatic interaction is controlled by the Coulomb interactions between point effective charges, because the investigated distances $y > 8\kappa_{\mathrm{B}}^{-1}$ and $x_2 - b_{\mathrm{col}} \sim 8\kappa_{\mathrm{B}}^{-1}$ are large compared both with the screening length κ_{B}^{-1} and the colloid diameter $\sigma_{\mathrm{col}} = 2.4\kappa_{\mathrm{B}}^{-1}$. In other words, $w_{\mathrm{col\ col}}$ at large distances y and $x - b_{\mathrm{col}}$ has the same functional form as in a primitive model where every charge is concentrated at the center of an impenetrable sphere. The ratio between the effective charge in the spherical-charge fluid and the effective charge in the point-charge model is expected to be of order unity, as indicated by the DLVO approximation (66) for the bulk effective charge, the renormalization of which is equal to 1.5 in the present experiment.

By virtue of Eq. (40), which is also valid in the presence of a surface charge on the wall (as discussed in Sec. V A), the screened potential $\phi(x,x',y)$ for point charges is the sum of a function with algebraic and exponential tails and of an exponentially decaying term $\phi_{\mathrm{sing}(i)}$ if x and x' are in the same subregion (i). As a consequence, we expect that $h_{\mathrm{col\ col}}(x,x',y)$ as well as the effective interaction $w_{\mathrm{col\ col}}(x,x',y)$ take different forms at distances shorter or larger than some distance $y_\star(x,x')$:

$$w_{\mathrm{col\ col}}(x,x',y) \underset{y_\star(x,x')<y}{\sim} \frac{f_{\mathrm{col\ col}}(x,x')}{y^3} \tag{69}$$

and

$$\frac{w_{\mathrm{col\ col}}(x,x',y)}{k_{\mathrm{B}}T} \underset{(\kappa_{\mathrm{B}}^{-1},\sigma_{\mathrm{col}})<y<y_\star(x,x')}{\sim} z_{\mathrm{col\ col}}(x,x')\tilde{\lambda}\frac{e^{-\tilde{y}}}{\tilde{y}}. \tag{70}$$

When $x = x'$ the distance $y_\star(x)$ from which the dipolar tail (69) becomes of the same magnitude order as the exponential tail (70) is estimated in the following. As checked in the following subsection, when the distance x from the wall increases, the range of distances $0 < y < y_\star(x)$, where the exponential tail in $w_{\mathrm{col\ col}}(x = x',y)$ overcomes its dipolar tail, also increases very fast, and the exponential tail tends to its repulsive bulk value,

$$z_{\mathrm{col\ col}}(x = x') \underset{(\kappa_{\mathrm{B}}^{-1},\sigma_{\mathrm{col}})<(x-b_{\mathrm{col}})}{\sim} [Z_{\mathrm{col}}^{\mathrm{eff\ B}}]^2. \tag{71}$$

In other words, for $(\kappa_{\mathrm{B}}^{-1},\sigma_{\mathrm{col}}) < y < y_\star(x)$ and $(\kappa_{\mathrm{B}}^{-1},\sigma_{\mathrm{col}}) < (x - b_{\mathrm{col}})$, $w_{\mathrm{col\ col}}(x = x',y)$ tends to the bulk value $w_{\mathrm{col\ col}}^{\mathrm{B}}(y)$ given in Eq. (68).

4. Linearized mean-field estimations

In a dilute system, because of the long-range of the Coulomb interaction, $w_{\mathrm{col\ col}}$ as well as $u_{\mathrm{col\ col}}$ are expected to decay at large distances as their mean-field values. The fast screening of the Coulomb interaction implies that, though bare Coulomb coupling between colloids is strong, the mean-field value of $w_{\mathrm{col\ col}}$ ($u_{\mathrm{col\ col}}$) at large relative distances is expected to be correctly given by linearizing functions of $\beta w_{\mathrm{col\ col}}$ ($\beta u_{\mathrm{col\ col}}$). (In the Mayer diagrammatic such a linearized mean-field theory is equivalent to a weak-coupling and high-dilution limit, as shown in Ref. [11]. The linearization is legitimate for purely ionic contributions.) Then

$$w_{\mathrm{col\ col}}^{LMF}(x,x',y) \underset{(\kappa_{\mathrm{B}}^{-1},\sigma_{\mathrm{col}})<y}{\sim} [Z_{\mathrm{col}}e]^2\phi(x,x',y), \tag{72}$$

where $\phi(x,x',y)$ is the solution of integral equation (21). If charges are not concentrated at points, the effect is contained in $\phi(x,x',y)$. According to general property (7), since x and x' are larger than $b_{\max} = b_{\mathrm{col}}$ for colloidal particles,

$$f_{\mathrm{col\ col}}^{LMF}(x,x') = [Z_{\mathrm{col}}e]^2\bar{D}_\phi(x)\bar{D}_\phi(x'). \tag{73}$$

If $b_{\mathrm{col}} \sim \sigma_{\mathrm{col}}/2$, then $b_{\mathrm{col}} \sim \kappa_{\mathrm{B}}^{-1}$ in the present experiment and, when x and x' are larger than κ_{B}^{-1}, $\bar{D}_\phi(x)$ is expected to have the same functional form as the potential $\bar{D}_{\phi^{(0)}}(x)$ calculated for point charges located at the centers of excluded-volume spheres and with uniform density profiles. ($\phi^{(0)}(x,x',y)$ takes into account the various closest approach distances to the wall b_α's; henceforth $\phi^{(0)}$ must not be confused with the potential $\phi^{(0)}$ written in Eq. (44) where all b_α's are equal to the same value b.) Therefore, we expect that for $y > y_\star^{LMF}(x)$

$$\frac{[Z_{\mathrm{col}}e\bar{D}_\phi(x)]^2}{y^3\,k_{\mathrm{B}}T} \underset{(\kappa_{\mathrm{B}}^{-1},\sigma_{\mathrm{col}})<(x-b_{\mathrm{col}})}{\sim} 2\frac{\epsilon_W}{\epsilon_{\mathrm{solv}}}\tilde{\lambda}[A_\phi Z_{\mathrm{col}}]^2\frac{e^{-2\kappa_{\mathrm{B}}(x-b_{\mathrm{col}})}}{\tilde{y}^3}, \tag{74}$$

where κ_{B}^{-1} is the same screening length as in the bulk. In the weak-coupling and high-dilution limit, at leading order $\kappa_{\mathrm{B}}^{(0)} = \kappa_D$. $A_\phi Z_{\mathrm{col}}$ is an effective charge that incorporates various effects. At leading order in the Coulomb-coupling and dilution parameters, $A_{\phi^{(0)}}$ is determined by the fact that all species have not the same approach distance to the wall and that charges are not concentrated at points. The first correction $A_{\phi^{(1)}}$ contains effects of the geometric repulsion and the electrostatic response of the wall, of its surface charge and of the nonuniform profile of the electrostatic potential created by the charge density profile in the vicinity of the wall. In fact, if the first correction $\phi^{(1)}$ is considered, then $w_{\mathrm{col\ col}}(x,x',y)$ itself must also be calculated at the same order and then other corrections arise from screened interactions mediated by colloids or ions. [The $1/y^3$ tail of $w_{\mathrm{col\ col}}^{(1)}(x,x',y)$ is calculated in the case of charges concentrated at points when there is no surface charge on the wall and when all charges have the same approach distance to the wall $b \ll \kappa_{\mathrm{B}}^{-1}$ in the forthcoming paper [12]. We check that the charge renormalization is not the same for the $1/y^3$ tail of $w_{\mathrm{col\ col}}^{(1)}(x,x',y)$ and for the exponential tail of $w_{\mathrm{col\ col}}^{\mathrm{B}\,(1)}(x - x',y)$.]

The distance $y_\star^{LMF}(x)$ at which the linearized mean-field dipolar tail (74) becomes of the same magnitude order as the exponential tail in Eq. (72) can be approximatively calcu-

lated as the distance $y_\star^{(0)}(x)$ at which the $1/y^3$ algebraic tail overcomes the exponential tails in $\phi^{(0)}$ defined in previous paragraph. The structure of $\phi^{(0)}$ at $x>b_{\max}$ and $x'>b_{\max}$ is the same as that in Eq. (44) where only the expression of $Z_{IV}^{(0)}(|\mathbf{k}|)$ depends on the fact that all b_α's are equal to the same value b or not. $y_\star^{(0)}(x)$ itself can be determined only roughly, because the $1/y^3$ term dominates all other algebraic tails in $\phi^{(0)}-\phi_{\text{sing}}^{(0)}$ at large y, but the exponential tails in $\phi^{(0)}-\phi_{\text{sing}}^{(0)}$ are not easy to estimate, as can be seen in a similar situation in Ref. [30]. We assume that the latter exponential tails are of the same order as $\phi_{\text{sing}}^{(0)}=\phi^{\text{D}}$ [see Eq. (28)] or negligible with respect to it. Then, if κ_D in $\phi^{(0)}$ is replaced by κ_{B}, an approximate value of $y_\star^{(0)}(x)$ is the solution of the equation

$$2\frac{\epsilon_W}{\epsilon_{\text{solv}}}e^{-2(\tilde{x}-\tilde{b}_{\text{col}})}=[\tilde{y}_\star^{(0)}(x)]^2e^{-\tilde{y}_\star^{(0)}(x)}, \tag{75}$$

where the tilde denotes dimensionless lengths defined as in Eq. (68). In the latter approximate equation we have replaced $A_{\phi^{(0)}}$ by 1, which is the case only when all closest approach distances b_α's to the wall are equal. When $\epsilon_W/\epsilon_{\text{solv}}$ is of order 1/80, $y_\star^{(0)}(x)$ is equal to $7\kappa_{\text{B}}^{-1}$ for $x=b_{\text{col}}$, $10\kappa_{\text{B}}^{-1}$ for $x-b_{\text{col}}=\kappa_{\text{B}}^{-1}$, $15\kappa_{\text{B}}^{-1}$ for $x-b_{\text{col}}=3\kappa_{\text{B}}^{-1}$, and $20\kappa_{\text{B}}^{-1}$ for $x-b_{\text{col}}=5\kappa_{\text{B}}^{-1}$.

In the experiment $x_2=9\kappa_{\text{B}}^{-1}$. If b_{col} is approximated by $b_{\text{col}}\sim\sigma_{\text{col}}/2\sim1.2\kappa_{\text{B}}^{-1}$, then $(x_2-b_{\text{col}})\sim8\kappa_{\text{B}}^{-1}$ and $y_\star^{(0)}(x_2)$ is far larger than the y's investigated. In other words, dipolar tail (74) is killed by the factor $\exp[-2\kappa_{\text{B}}(x_2-b_{\text{col}})]=\exp(-16)\sim10^{-7}$ and the exponential tail in Eq. (72) dominates algebraic tail (74) in the range of investigated y's.

5. Experimental results in the vicinity of a single wall

At the finite distance $x_2\sim9\,\kappa_{\text{B}}^{-1}$ from the wall, $w_{\text{col col}}$ is again measured in the range of y's from $8\kappa_{\text{B}}^{-1}$ to $25\kappa_{\text{B}}^{-1}$. At short distances, $w_{\text{col col}}$ is repulsive and decreases when y increases, its sign changes at $y=y_{\text{inv}}\sim9\kappa_{\text{B}}^{-1}$, $w_{\text{col col}}$ has a negative minimum at $y_{\min}\sim13\,\kappa_{\text{B}}^{-1}$, and its dependance on y for large y's is compatible with an algebraic law.

In the range $8\kappa_{\text{B}}^{-1}<y<y_{\text{inv}}\sim9\kappa_{\text{B}}^{-1}$ where $w_{\text{col col}}$ is repulsive, the experimental curve is fitted by the exponentially fast bulk decay (64),

$$w_{\text{col col}}(x=x',y)\underset{y<y_{\text{inv}}}{\sim}w_{\text{col col}}^{B}(x=x',y). \tag{76}$$

If $b_{\text{col}}\sim\sigma_{\text{col}}/2$, result (76) is in agreement with the linearized mean-field approach of the preceding subsection: the exponential tail in the electrostatic pairwise interaction (72) dominates the repulsive dipolar tail in the whole range of investigated y. Moreover, it is well approximated by its repulsive bulk value, as argued after Eq. (71).

Therefore, the origin of the attraction measured in experiment [2] for $y>y_{\text{inv}}$ is not electrostatic interaction at equilibrium. The granted explanation for the observed attraction near one wall relies on a hydrodynamical effect involving electrostatic interactions. Squires and Brenner [3] argued that the experimental curve could be accounted for by the competition between the exponential tail of the effective electrostatic interaction and the hydrodynamical force induced between colloids by the external electrostatic field created by the surface charge on the wall. This interaction is attractive if the surface charge on the wall has the same sign as the colloid charge, which is indeed the case in the experiment where the surface charge on the wall is negative as the charges carried by colloids. Squires and Brenner calculated the interaction between the surface charge and a colloid in a bath of ions by using a linearized mean-field approach with point charges, namely, by using the same approximations as those used in the preceding subsection for the equilibrium effective electrostatic interactions. For the effective charge near the wall they took the bulk DLVO expression. For the sake of completeness, we rewrite their result where we replace κ_D^{ion} by the effective inverse screening length κ_{B}:

$$\frac{u_{\text{col col}}^{\text{hyd}}}{k_{\text{B}}T}=-\frac{\tau}{1+(\kappa_{\text{B}}\sigma_{\text{col}}/2)}[Z_{\text{col}}e]^2\tilde{\lambda}\frac{6(x/\sigma_{\text{col}})^2}{(x/\sigma_{\text{col}})-(9/32)}\times\frac{\tilde{x}^2}{[4\tilde{x}^2+\tilde{y}^2]^{3/2}}e^{-[\tilde{x}-(\tilde{\sigma}_{\text{col}}/2)]}. \tag{77}$$

In Eq. (77) τ is the ratio between the surface charge density on the wall and the surface density of the charge $Z_{\text{col}}e$ on a colloidal sphere. Squires and Brenner showed that Brownian dynamics simulations account for experimental curves when $\tau=0.4$. (The latter value of τ can be explained on purely geometrical grounds in a phenomenological theory of effective-charge saturation [31].) When τ is set to 0.4, the magnitude order of $u_{\text{col col}}^{\text{hyd}}$ is larger than the electrostatic exponential tail (76) when $y>9\kappa_{\text{B}}^{-1}$.

C. Open questions

As a conclusion, the lightning from statistical mechanics of charge fluids at equilibrium to the question at the end of Sec. VI A is the following.

First, the observed attraction between dilute colloidal particles in the vicinity of a single wall cannot arise from purely electrostatic effects if the linearized mean-field scheme for $w_{\text{col col}}$ is valid, as it is the case in previous mean-field theories for $u_{\text{col col}}$.

For the distances investigated in the experiment of Ref. [2], the exponential tail prevails over the algebraic tail. However, we stress that the magnitude order of the coefficient $f_{\text{col col}}(x,x')$ in the $1/y^3$ tail of $w_{\text{col col}}(x,x',y)$ is very sensitive to the actual value of the closest approach distance b_{col} of colloids to the wall, as it is the case for its linearized mean-field value. If dilute silica spheres were used instead of polystyrene sulphate spheres, the former denser colloidal particles might sediment in a plane parallel to the glass plate, as it is the case in the experiment [27]. (We recall that in the experiment [27], silica colloids are not dilute and results of Secs. VI B 3 and VI B 4 cannot be applied.) Then, although *all* colloids would be constrained to lie in the plane at x_{bal} by the balance between gravity and the interaction with the wall surface charge, the exponential screening in the direction x perpendicular to the wall would still be ensured by the pres-

ence of ions of both signs in the solution. (The localization of colloidal particles in a plane does not cause qualitative changes in the electrostatic screening contrarily to what happens at an air-water interface [30].) In this case, b_{col} would be equal to x_{bal}, the only accessible distance x for colloids, and the repulsive dipolar tail (74) at $x=x_{\mathrm{bal}}$ would dominate the exponential tail in Eq. (72) in a range that can be estimated to be $y>y_{\star}^{(0)}(x=b_{\mathrm{col}})\sim 7\kappa_{\mathrm{B}}^{-1}$.

If coupling or steric effects at higher density were such that the linearized mean-field approximation (72) failed, then the coefficient $f_{\mathrm{col\ col}}(x,x')$ in the $1/y^3$ tail of $w_{\mathrm{col\,col}}$ would no longer have the dipolar structure (73) and its sign might vary. In the case of the bulk effective interaction $w^{\mathrm{B}}_{\mathrm{col\ col}}$, such coupling and steric effects have been investigated by means of approximate closures of the integral Ornstein-Zernicke equations for the primitive model [32,33].

On the other hand, in the experiment of Ref. [4], where colloids are densely distributed and confined between two glass walls separated by a distance equal to only a few colloid diameters, Han and Grier exclude any explanation for the observed attraction that would be based on kinematic effects, such as a hydrodynamic coupling. (The latter effect, which disappears for symmetry reasons when colloids lie exactly at the same distance from two equally charged surfaces, may arise because experiments necessarily have a degree of off center. However, typical drift speeds in the experiment of Ref. [4] are far too small to mediate measurable in-plane hydrodynamic coupling.)

We stress that in the case of a solution confined between two plates carrying external negative charges, boundary conditions are changed and the arguments used in Sec. III no longer hold. Without any further investigation, we cannot assert whether the $f_{\phi}(x,x')/y^3$ tail of $\phi(x,x',y)$ is still repulsive everywhere in the fluid and we expect that $f_{\phi}(x,x')$ no longer has factorized structure (7). We notice that, in an approximated calculation where density profiles are uniform between two plates [8], $f_{\phi^{(0)}}(x,x')$ loses factorization property (7), but it is still repulsive.

Finally, we notice that the electrostatic model with pure charge-charge Coulomb forces is perhaps too crude. It does not take into account the polarization of the solvent around each colloidal particle. The latter intricate phenomenon might be the root of the observed attraction between like-charge colloids.

ACKNOWLEDGMENTS

We are indebted to J.-M. Caillol, D. Levesque, E. Trizac, and J.-J. Weis for fruitful discussions.

APPENDIX

In the present Appendix, we use the principles recalled at the beginning of Sec. IV B in order to determine the formal structure of the $1/y^3$ tail of the Ursell function $h_{\alpha\alpha'}(x,x',\mathbf{y})$, when all species have the same closest approach distance to the wall. In this case the $1/y^3$ tail of the bond F^{cc} has dipolar structure (7) of the screened potential ϕ

$$F^{\mathrm{cc}}(x,x',\mathbf{y}) \underset{y\to+\infty}{\sim} -\frac{\beta e^2}{\epsilon_{\mathrm{solv}}} Z_{\alpha} Z_{\alpha'} \frac{\bar{D}_{\phi}(x)\bar{D}_{\phi}(x')}{y^3}. \quad \text{(A1)}$$

The $1/y^3$ tail of $h^{--}_{\alpha\alpha'}(x,x',\mathbf{y})$ is the sum of the tails of all graphs $h^{--}_{m}(a,a')$ with m bonds F^{cc} ($m=1,2,\ldots$). The $1/y^3$ tail of $h^{--}_{m}(a,a')$ itself is the sum of the m tails arising from every bond F^{cc} in h^{--}_{m} by virtue of Eq. (61). With the notations of definition (33), the pth bond F^{cc} in h^{--}_{m} ($p=1,\ldots,m$) in Fig. 3 links points $(p-1)'=(\mathbf{r}'_{p-1},\gamma'_{p-1})$ and $p=(\mathbf{r}_p,\gamma_p)$. [With notations of Fig. 3 $(\mathbf{r}'_0,\gamma'_0)=c$ and $(\mathbf{r}_m,\gamma_m)=c'$.] According to Eq. (60), the tail arising from the pth bond F^{cc} in $h^{--}_{m}(a,a')$ reads

$$-\frac{\beta e^2}{\epsilon_{\mathrm{solv}}}\frac{1}{y^3} C^{--\,[p-1]}_{\alpha}(x) C^{--\,[m-p]}_{\alpha'}(x'). \quad \text{(A2)}$$

In Eq. (A2) $C^{--\,[m-p]}_{\alpha'}(x')$ denotes the contribution from the part of h^{--}_{m} between points $p=(\mathbf{r}_p,\gamma_p)$ and $a'=(\mathbf{r}',\alpha')$. This part contains $m-p$ bonds F^{cc} and

$$C^{--[m-p]}_{\alpha'}(x') \equiv \int dx_p \sum_{\gamma_p} \rho_{\gamma_p}(x_p) Z_{\gamma_p} \bar{D}_{\phi}(x_p) \times h^{--}_{m-p}(x_p,x',\mathbf{k}=\mathbf{0};\gamma_p,\alpha'). \quad \text{(A3)}$$

The contribution from the part of h^{--}_{m} between points $a=(\mathbf{r},\alpha)$ and $(p-1)'=(\mathbf{r}'_{p-1},\gamma'_{p-1})$ is equal to the rhs of Eq. (A3), where (x_p,γ_p) is replaced by (x'_{p-1},γ'_{p-1}) while $h^{--}_{m-p}(x_p,x',\mathbf{k}=\mathbf{0};\gamma_p,\alpha')$ is replaced by $h^{--}_{p-1}(x,x'_{p-1},\mathbf{k}=\mathbf{0};\alpha,\gamma'_{p-1})$. We have used the same notation for both contributions, because $h^{--}_{p-1}(a,(p-1)')$ is symmetric with respect to a and $(p-1)'$. The $1/y^3$ tail of $h^{--}_{\alpha\alpha'}(x,x',\mathbf{y})$ is equal to

$$-\frac{\beta e^2}{\epsilon_{\mathrm{solv}}}\frac{1}{y^3}\sum_{m=1}^{+\infty}\sum_{p=1}^{m} C^{--[p-1]}_{\alpha}(x) C^{--[m-p]}_{\alpha'}(x'). \quad \text{(A4)}$$

The double sum in expression (A4) can be written as a product of two sums with the result

$$h^{--}_{\alpha\alpha'}(x,x',\mathbf{y}) \underset{y\to+\infty}{\sim} -\frac{\beta e^2}{\epsilon_{\mathrm{solv}}}\frac{1}{y^3} C^{--}_{\alpha}(x) C^{--}_{\alpha'}(x') \quad \text{(A5)}$$

with $C^{--}_{\alpha}(x)\equiv\Sigma_{n=0}^{+\infty} C^{--[n]}_{\alpha}(x)$. By virtue of Eq. (A3),

$$C^{--}_{\alpha}(x) = \int d\mathbf{r}'' \sum_{\gamma''} \rho_{\gamma''}(x'') Z_{\gamma''} \bar{D}_{\phi}(x'') h^{--}_{\alpha\gamma''}(\mathbf{r},\mathbf{r}''). \quad \text{(A6)}$$

The $1/y^3$ tail of $h^{c-}_{\alpha\alpha'}(x,x',\mathbf{y})$ appears as the sum of two contributions, as it is the case for every h^{c-}_{m} when $m\geqslant 2$. The

$1/y^3$ tail arising from the bond F^{cc} attached to a in $h_m^{c^-}(a,a')=h_m^{c^-}(x,x',\mathbf{y};Z_\alpha,Z_{\alpha'})$ is equal to

$$-\frac{\beta e^2}{\epsilon_{solv}}\frac{1}{y^3}Z_\alpha \bar{D}_\phi(x)C_{\alpha'}^{-\,-[m-1]}(x') \tag{A7}$$

with the same notation as in expression (A2). When $m=1$, expression (A7) is the only contribution. When $m\geqslant 2$, the $1/y^3$ tail that originates from the other $m-1$ bonds F^{cc} is the sum

$$-\frac{\beta e^2}{\epsilon_{solv}}\frac{1}{y^3}Z_\alpha \sum_{p=2}^{m}\bar{C}^{c-[p-1]}(x)C_{\alpha'}^{-\,-[m-p]}(x'). \tag{A8}$$

In Eq. (A8) we have exhibited the fact that the dependence on Z_α in h^{c^-} is merely a multiplicative factor Z_α: we have defined $Z_\alpha \bar{C}^{c-[p-1]}(x)$ similarly to $C_\alpha^{-\,-[p-1]}(x)$ with $h_{p-1}^{c^-}$ in place of h_{p-1}^{--} [see the comment after Eq. (A3)]. After summation over m from 1 to $+\infty$, we get

$$h_{\alpha\alpha'}^{c^-}(x,x',\mathbf{y}) \underset{y\to+\infty}{\sim} -\frac{\beta e^2}{\epsilon_{solv}}\frac{1}{y^3}Z_\alpha[\bar{D}_\phi(x)+\bar{C}^{c^-}(x)]C_{\alpha'}^{-\,-}(x'), \tag{A9}$$

with $\bar{C}^{c^-}(x)\equiv\Sigma_{n=1}^{+\infty}\bar{C}^{c-\,[n]}(x)$. Similar to Eq. (A6)

$$Z_\alpha \bar{C}_\alpha^{c^-}(x)=\int d\mathbf{r}''\sum_{\gamma''}\rho_{\gamma''}(x'')Z_{\gamma''}\bar{D}_\phi(x'')h_{\alpha\gamma''}^{c^-}(\mathbf{r},\mathbf{r}''). \tag{A10}$$

The asymptotic tail of $h_{\alpha\alpha'}^{-c}$ takes a form similar to that of $h_{\alpha\alpha'}^{c^-}$: the roles of α and α' are exchanged and there appears a $\bar{C}^{-c}(x')$ defined by analogy with $\bar{C}^{c^-}(x)$ with $h_{\gamma''\alpha'}^{-c}(\mathbf{r}'',\mathbf{r}')$ in place of $h_{\alpha\gamma''}^{c^-}(\mathbf{r},\mathbf{r}'')$. Since $h_{\gamma''\alpha'}^{-c}(\mathbf{r}'',\mathbf{r}')=h_{\alpha'\gamma''}^{c^-}(\mathbf{r}',\mathbf{r}'')$, $\bar{C}^{-c}(x')=\bar{C}^{c^-}(x')$.

The calculation of the $1/y^3$ tail of $h_{\alpha\alpha'}^{cc}(x,x',\mathbf{y})$ is a generalization of the previous one. Four kinds of contributions can be distinguished, according to whether the $1/y^3$ tail of $h_m^{cc}(a,a')$ arises or not from the bond F^{cc} attached to x or from the bond F^{cc} attached to x'. We obtain

$$h_{\alpha\alpha'}^{cc}(x,x',\mathbf{y}) \underset{y\to+\infty}{\sim} -\frac{\beta e^2}{\epsilon_{solv}}\frac{1}{y^3}Z_\alpha Z_{\alpha'}[\bar{D}_\phi(x)+\bar{C}^{c^-}(x)] \times[\bar{D}_\phi(x')+\bar{C}^{c^-}(x')]. \tag{A11}$$

After summation of tails (A5), (A9) and the symmetric one, together with tail (A11), the large-y behavior of $h_{\alpha\alpha'}(x,x',\mathbf{y})$ proves to have dipolar structure (8) where $D_\alpha(x)$ is given in Eq. (62).

[1] J.P. Hansen and I.R. McDonald, *Theory of Simple Liquids* (Academic, London, 1976).
[2] A.E. Larsen and D.G. Grier, Nature (London) **385**, 30 (1997).
[3] T. Squires and M.P. Brenner, Phys. Rev. Lett. **85**, 4976 (2000).
[4] Y. Han and D.G. Grier, Phys. Rev. Lett. **91**, 038302 (2003).
[5] Ph.A. Martin, Rev. Mod. Phys. **60**, 1075 (1988).
[6] B. Jancovici, J. Stat. Phys. **28**, 43 (1982).
[7] A.S. Usenko and I.P. Yakimenko, Sov. Tech. Phys. Lett. **5**, 549 (1979).
[8] S.L. Carnie and D.Y.C. Chan, Mol. Phys. **51**, 1047 (1984).
[9] B. Jancovici, J. Stat. Phys. **29**, 263 (1982).
[10] J.-N. Aqua and F. Cornu, J. Stat. Phys. **97**, 173 (1999).
[11] J.-N. Aqua and F. Cornu, J. Stat. Phys. **105**, 211 (2001).
[12] J.-N. Aqua and F. Cornu (unpublished).
[13] E. Meeron, J. Chem. Phys. **28**, 630 (1958); *Plasma Physics* (McGraw-Hill, New York, 1961).
[14] J.-N. Aqua and F. Cornu, J. Stat. Phys. **105**, 245 (2001).
[15] D.A. McQuarrie, *Statistical Mechanics* (Harper & Row, New York, 1973).
[16] J.D. Jackson, *Classical Electrodynamics* (Wiley, New York, 1962).
[17] A. Alastuey, F. Cornu, and A. Perez, Phys. Rev. E **49**, 1077 (1994); F. Cornu, *ibid.* **53**, 4562 (1996).
[18] F. Cornu and Ph.A. Martin, Phys. Rev. A **44**, 4893 (1991).
[19] F. Cornu, Phys. Rev. E **53**, 4595 (1996).
[20] L.S. Brown and L.G. Yaffe, Phys. Rep. **340**, 1 (2001).
[21] D. Zwillinger, *Handbook of Differential Equations* (Academic Press, New York, 1989).
[22] I.M. Gel'fand and G.E. Shilov, *Generalized Functions* (Academic, New York, 1964), Vol. 1.
[23] D.F. Evans and H. Wennerström, *The Colloidal Domain (where Physics, Chemistry, Biology and Technology Meet)* (VCH Publishers, New York, 1994).
[24] E.J.W. Verwey and J.Th.G. Overbeek, *Theory of the Stability of Lyophobic Colloids* (Dover, New York, 1999).
[25] J.C. Neu, Phys. Rev. Lett. **82**, 1072 (1999); J.E. Sader and D.Y. Chan, J. Colloid Interface Sci. **213**, 268 (1999); J.E. Sader and D.Y. Chan, Langmuir **16**, 324 (2000).
[26] E. Trizac, Phys. Rev. E **62**, R1465 (2000).
[27] S.H. Behrens and D.G. Grier, Phys. Rev. E **64**, 050401 (2001).
[28] R. Kjellander and D.J. Mitchell, Chem. Phys. Lett. **200**, 76 (1992).
[29] J.-P. Hansen and H. Löwen, Annu. Rev. Phys. Chem. **51**, 209 (2000).
[30] A.J. Hurd, J. Phys. A **18**, L1055 (1985).
[31] L. Bocquet, E. Trizac, and M. Aubouy, J. Chem. Phys. **117**, 8138 (2002).
[32] M. Medina-Noyola and D.A. McQuarrie, J. Chem. Phys. **73**, 6279 (1980).
[33] M.D. Carbajal-Tinoco, F. Castro-Román, and J.L. Arauz-Lara, Phys. Rev. E **53**, 3745 (1996); P. González-Mozuelos and M.D. Carbajal-Tinoco, J. Chem. Phys. **109**, 11074 (1998); M.D. Carbajal-Tinoco and P. González-Mozuelos, *ibid.* **117**, 2344 (2002).